NTNU – Trondheim
Norwegian University of
Science and Technology

Reservoir Management under Uncertainty

Lars Skjærpe Midttun

Master of Science in Cybernetics and Robotics
Submission date: June 2015
Supervisor: Bjarne Anton Foss, ITK

Norwegian University of Science and Technology
Department of Engineering Cybernetics

NTNU
Norwegian University of Science and Technology

Faculty of Information Technology, Mathematics and Electrical Engineering

Department of Engineering Cybernetics

Master Thesis

Name of candidate: Lars Skjærpe Midttun

Subject: Engineering Cybernetics

Title: Reservoir management under uncertainty

In the operation of oil and gas systems, optimization is employed to enhance the performance. This is often denoted as Real Time Optimization (RTO), and has gained increasing attention the last decade. In RTO, some sort of model of the system is used to predict the outcome when altering the decision variables. These predictive models are however subject to uncertainty. This is due to the complexity of the system and lack of measurements. We can never obtain an exact representation of the subsurface reservoir and multiphase flow is inherently difficult to model.

In reservoir management, uncertainty is often ignored, or incorporated by using multiple model realizations to represent the uncertainty. There is little work on incorporating output constraints when considering multiple realizations. The published work which do include output constraints, treat them in a robust fashion. This implies that the solution must satisfy the output constraints at all future time steps, for all realizations, leading to an overly conservative solution. In this work, output constraints should be handled in a probabilistic way, leading to less conservative solutions in which the conservativeness can be controlled.

Task description:

1. Perform a literature review on reservoir management under uncertainty
2. Perform a case study on reservoir optimization
   a. In a deterministic setting
   b. Using multiple realizations with no output constraints

If there is time, the case study should also include

   c. Using multiple realizations with output constraints in a robust fashion
   d. Using multiple realizations with probabilistic output constraints

Starting date:
10.01.2015

End date:
10.06.2015

Co-supervisor: PhD student Kristian G. Hanssen, NTNU

Trondheim,

Bjarne Foss
Professor/supervisor

Summary

Uncertainty poses a major concern in reservoir management. To maximize production, engineers and geoscientists use numerical models of the reservoir to simulate the production process in advance, and mathematical optimization is used to find an optimal recovery strategy. However, acquiring an accurate description of a subsurface hydrocarbon reservoir is impossible, and hence these models are highly susceptible to uncertainty. With uncertainties present in the model, it is hard to know what the optimal production configuration is, as the actual outcome might be different from the prediction. The standard approach to this issue is to use the expected values of the uncertain parameters when solving the optimization problem, which basically ignores the uncertainty.

This thesis addresses the uncertainty problem in reservoir management. A methodology for handling optimization problems containing uncertain parameters, called stochastic programming, is introduced. The reservoir control optimization problem is formulated using this framework, and it is argued for why it is necessarily better than a regular deterministic formulation. A case study regarding a realistic reservoir model with uncertainties is carried out, showing how the stochastic solution yields higher expected return and fewer constraint violations than the deterministic solution. Moreover, it is explained how stochastic programming can be used to control risk when making decisions based on uncertain information.

Sammendrag

En stor utfordring innenfor olje- og gassproduksjon er usikkerhet. For å sikre maksimal utvinning bruker petroleumsingeniørene numeriske modeller av reservoaret til å simulere produksjonen på forhånd, og ved hjelp av matematisk optimalisering bestemmes en optimal utvinningsstrategi. Det er derimot umulig å lage en korrekt kunstig fremstilling av et oljereservoar som befinner seg flere kilometer under havbunnen, altså er disse modellene sterkt beheftet med usikkerhet. Usikkerhet gjør det vanskelig å bestemme en optimal konfigurasjon av produksjonssystemet, ettersom virkeligheten kan være noe helt annet enn det modellene tilsier. En vanlig måte å håndtere dette på er å bruke forventningsverdiene til de usikre parameterne, men sannheten er at denne metoden ignorerer usikkerheten.

Denne oppgaven tar for seg usikkerhetsproblemet i reservoaroptimalisering, eng. reservoir management. Leseren introduseres for en metodikk som kan brukes til å håndtere optimaliseringsproblemer med usikre parametere, kalt stokastisk programmering. Dette rammeverket brukes til å formulere et produksjonsoptimaliseringsproblem, hvor det argumenteres for hvorfor dette nødvendigvis er bedre enn en standard deterministisk formulering. I et realistisk case-studie som tar for seg en usikker reservoarmodell, vises det at den stokastiske løsningen gir bedre avkastning og færre brudd på begrensningene enn den deterministiske løsningen. Videre forklares det hvordan stokastisk programmering kan brukes til å kontrollere risiko i en beslutningsprosess basert på usikker informasjon.

Preface

This document is the author's final master's thesis at the Department of Engineering Cybernetics at the Norwegian University of Science and Technology, carried out during the spring semester of 2015. The given task followed from a project assignment conducted in the autumn semester of 2014.

Readers of this report are assumed to have a higher education in a technical field, with basic understanding of optimization theory and statistical analysis. No specific knowledge of oil and gas production is required, but is considered an advantage for understanding the entirety of this report.

I will like to thank my co-supervisor, PhD student Kristian G. Hanssen, for valuable feedback and teaching through the whole school year. Furthermore, a big thanks goes out to PhD student Andres Codas. Without his guidance and desire to help, the results in this work would not have been achieved. I would also like to thank my supervisor, professor Bjarne Foss, for follow-up and motivational feedback from his temporary residence in Brazil.

Trondheim, June 10, 2015

Lars Skjærpe Midttun

Contents

List of Figures

Chapter 1

Introduction

1.1 Background

The petroleum sector is the largest industry in the world in terms of dollar value. Not only is fossil fuels the world's most important energy source, oil is also the feedstock of a wide range of chemical products that are critical in today's society. Since the discovery of the Ekofisk field in the North Sea in 1969, oil and gas has been Norway's main source of income, and is by many considered to be the cornerstone of the nation's welfare state. Over a 40 year period the oil and gas industry has created values worth today's equivalent of 10 000 billion NOK, and in 2013 the industry alone stood for 22 % of the added value in the country.[1]

In light of these numbers, huge sums are invested in the development of petroleum technology. A lot of the research is aimed at improving extraction strategies for subsurface oil reservoirs, usually referred to as reservoir management, as there are big potential savings and earnings from improving production by even just a little. This area of research has made mathematical optimization find its way into petroleum engineering, merging the fields of classical geosciences and cy-

[1] Figures are collected from www.regjeringen.no

bernetics into what we call reservoir control optimization.

Uncertainty poses a major concern in oil and gas production. The production configuration is based on geological models that are highly susceptible to uncertainty, thus it is crucial to handle this effectively. To maximize production, the system will often be operating on its processing capacity constraints. If the controller setpoints used to achieve this come from solving a mathematical optimization problem containing uncertain parameters, the constraints might actually be violated without anyone knowing. This can result in increased wear on equipment and eventually failure, which again poses a safety issue. Moreover, constraint violations could also cause the system to unnecessarily underperform. All in all, it is very difficult to make informed decisions under uncertain conditions.

Handling uncertainty in oil and gas production is receiving increased attention, for several reasons. Stricter requirements to health, safety and environment make it totally necessary to account for uncertainty, and not to mention, be aware of *where* the uncertainties appear in the system. As in all sectors, there is also big interest in being able to monitor and control *risk*, both financial and safety related. As seen from the downturn in the oil and gas industry at the time of writing, the uncertain market has huge impacts on the companies who make a living of it.

1.2 Objective

This work addresses how uncertainty can be incorporated in reservoir management. The focus is given to the uncertainties related to the geological models used for conducting the reservoir control optimization. The reader is introduced to the framework that deals with optimization under uncertainty, called stochastic programming, and how this can be applied to oil and gas production optimization. The aim is to give the reader an overlying understanding of how uncertainty can be explicitly included in a mathematical optimization problem, how this differs from regular deterministic optimization, and to convey the main advantages of using such an approach. The thesis also serves as a theoretical introduction to reservoir simulation.

Several challenges come up when including uncertainty. First of all, uncertainty is represented using stochastic (random) variables that must be treated differently from deterministic variables. Moreover, evaluating stochastic functions often lead to extensive computations, e.g. multidimensional integrals. There is also no straight forward way of extending a deterministic optimization problem to include uncertainty, thus formulating a stochastic programming problem can be difficult.

1.3 Previous work

Regarding earlier literature, a fair amount of research has been made to reservoir management under uncertainty. However, most of it is related to decision making in long-term field planning, and the theory is often adapted from portfolio analysis. Less work is available on incorporating uncertainty directly in reservoir control optimization. When there is uncertainty in the geological model, it has become fairly standard to visualize this using multiple realizations, but these are rarely included all the way through the mathematical optimization.

1.4 Structure of the report

The thesis report is structured as follows. Ch. 2 introduces the reader to reservoir simulation, explaining how it is done and why it is important. The reservoir management concept is elaborated on in Ch. 3, and the stochastic programming framework for optimization under uncertainty is introduced and linked to the reservoir optimal control problem. Ch. 4 gives a literature review on previous work done on reservoir management under uncertainty. In Ch 5, the theory in Ch. 3 is applied in a realistic case study to promote the strength of stochastic programming and its wide area of application.

Chapter 2

Introduction to Reservoir Simulation

For an Exploration & Production (E&P) company, the phase between the discovery of a possible hydrocarbon reservoir and the actual drilling and subsequent production is critical. The company needs to analyze and evaluate the chance of success, as the cost of drilling a well is in the hundred million dollar class, thus the prize of making a mistake is high. They also need to determine how much oil they can expect to extract from the reservoir, and decide whether it will be profitable to produce it. After the production has started, the engineers and geoscientists must analyze the development in the reservoir in order to maintain maximal oil recovery. In order to conduct these analyzes the company uses advanced simulation tools to visualize the subsurface conditions. This is called reservoir simulation, and is considered to be one of the most important engineering areas in the E&P sector. This chapter covers the most basic parts of reservoir simulation. The target is to convey the main purposes and explain the central building blocks in the implementation.

2.1 What is reservoir simulation?

Reservoir simulation is a technique where a numerical model is used to describe a hydrocarbon reservoir's geological and petrophysical properties, with the purpose of predicting dynamic behavior in the reservoir over time. Reservoir simulation is one of the most important tools for supporting reservoir management, i.e., to maintain an optimal configuration of the production facilities to maximize oil recovery (see Ch. 3).

2.2 Building a geological model

Creating a numerical model of a petroleum reservoir is a highly extensive task, and requires collection and interpretation of a multitude of information. Obtaining geophysical data requires careful planning and can be very time consuming. Furthermore, the information must be transferred to the model in an efficient manner.

2.2.1 Data gathering

Seismic surveys play an important role in identifying the extent of the reservoir and recognizing rock layers. Seismic data can also help naming the rock types in the reservoir and identifying fractures and faults. However, shooting seismic surveys is expensive and time consuming, and the resolution is limited (usually in the ten meters scale, Lie (2014)). Well logs are carried out by lowering various measuring tools into the wells, and provide very accurate information. The main drawback is that the information is valid only in a certain vicinity of the wells. Collecting core samples from the reservoir can be used to verify measurements, but suffers from the same downside as well logs. By combining information from all of these utilities, the engineers can start developing an artificial replica of the real reservoir, carefully choosing the data they consider to be the most reliable. If available, they can enhance the information received from measurements by looking at the production history of the particular field, and run well tests. Everything contributes to the big puzzle, but it is quite obvious that obtaining an exact representation of the whole reservoir is impossible. Large uncertainties are attached to the numerical model, as will be further discussed in Ch. 3.

2.2.2 Discretization

A reservoir model must link the geological and petrophysical data to the reservoir geometry. To make this doable, the reservoir model is discretized in space and represented as a volumetric grid. Each cell in the grid is considered a *representative elementary volume* (REV), in which all rock and fluid properties (see Sections 2.3-2.4) are fixed in space, meaning they are the same for the whole cell (they can still change with time). The REV principle is illustrated in Figure 2.1. The information gathered as discussed in Section 2.2.1 is used to populate the different cells in the grid, thus resulting in complete reservoir description. The process of assigning parameter values to the grid cells is a challenging process, as local measurements must be upscaled to grid size. This introduces uncertainty, which is the topic of Ch. 3. With the grid filled up, the simulator uses the information to solve fundamental differential equations across the cells. These equations arise from physical laws, e.g. conservation of mass (the continuity equation), Darcy's law (the equation of flow) and pressure-volume or pressure-density relationships (the equation of state), and must be discretized in time and space to fit the grid structure. Given boundary conditions, the equations are solved for every time step in a given horizon, creating a picture of how fluids flow within the reservoir. This is explained in detail in Section 2.5.

2.2.3 Grid types

There are many ways to design a grid, and the choice is usually a trade-off between accuracy and computational efficiency. According to Lie and Mallison (2013), the most widely used grid type in industrial applications is the stratigraphic grid, which is designed to emphasize that the majority of reservoirs consist of several sediment layers. The layers, often called beds, have usually been subject to different wear and erosion, leading to fractures and faults, and the stratigraphic grid is meant to capture this in a clear manner. The most common form of stratigraphic grids is the corner-point grid. A corner-point grid uses hexahedronal cells that are aligned such that they can be numbered using logical (i, j, k) notation. Figure 2.2a and 2.2b show corner-point grids in two and three dimensions, respectively. Notice the five distinct faults in Figure 2.2a. Another type of stratigraphic grid with increasing popularity is the unstructured Perpendicular Bisector (PEBI) grid. Cells in a PEBI grid can have any shape and can be arranged to fit any reservoir geometry. The cells can also be refined in areas where a special orientation is needed, for example around a well, as displayed in Figure 2.3.

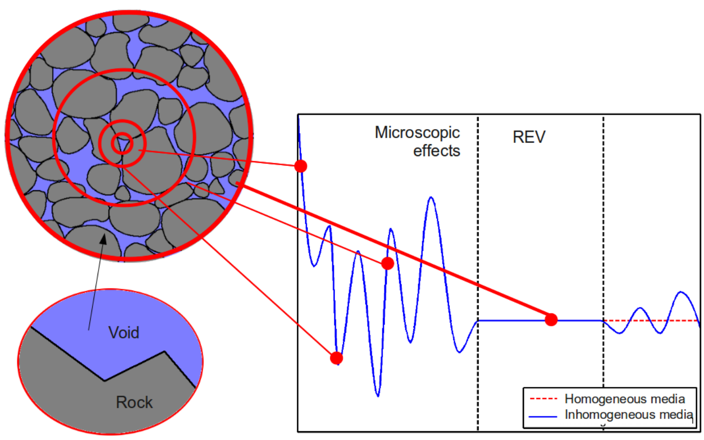

Figure 2.1: Rock properties such as porosity are assumed constant within a REV (Lie and Mallison, 2013)

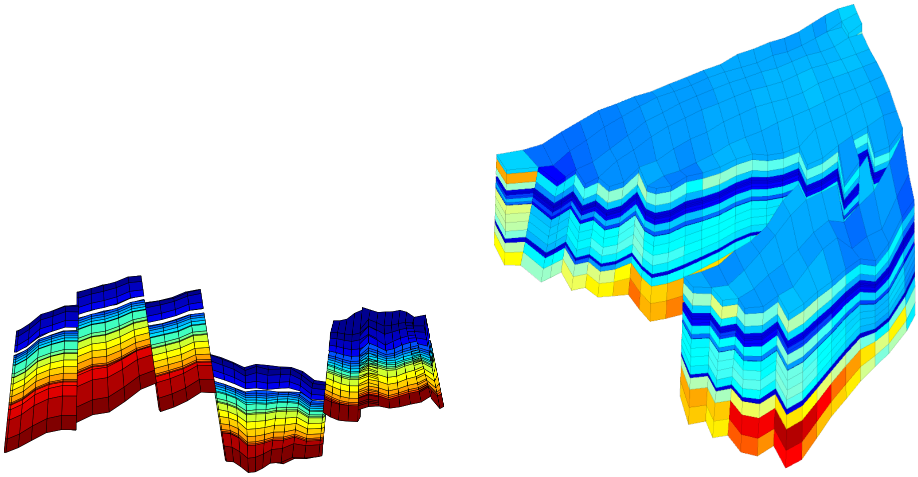

(a) 2D corner-point grid
(b) 3D corner-point grid

Figure 2.2: Reservoirs modeled with corner-point grids (Lie, 2014)

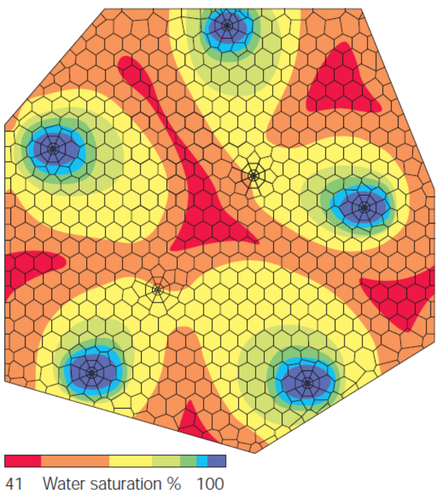

Figure 2.3: PEBI grid with local refinement around wells (Adamson and Crick, 1996)

2.3 Rock properties

A hydrocarbon reservoir is a subsurface area of porous rocks having oil and/or gas trapped within the pores. The rocks have many properties that affect how fluids flow inside the reservoir, thus these are important to obtain and include in the model. This section covers the most central rock properties when working with reservoir modeling.

2.3.1 Porosity

Porosity is a dimensionless quantity defined as the fraction of the bulk volume that is occupied by pores (voids), i.e., the volumetric void space in the rock. Porosity is usually assigned the letter ϕ, and is related to a material's compressibility in the following way:

$$c_r = \frac{1}{\phi}\frac{\mathrm{d}\phi}{\mathrm{d}p} = \frac{\mathrm{d}\ln(\phi)}{\mathrm{d}p} \tag{2.1}$$

where c_r is the compressibility and p is the overall reservoir pressure (Lie, 2014). If the compressibility can be assumed to be constant, Eq. (2.1) can be solved for the porosity to obtain

$$\phi(p) = \phi_0 e^{c_r(p-p_0)} \tag{2.2}$$

It is also common to use a linearization of Eq. (2.2), giving (Lie, 2014)

$$\phi(p) = \phi_0\left[1 + c_r(p - p_0)\right] \tag{2.3}$$

In a porous reservoir rock, the void space may be filled with water, oil or gas, thus the porosity is directly proportional to production potential. This is why porosity is considered one of the most crucial parameters when exploring a reservoir. Porosity cannot be measured directly, but must be estimated from other measurable quantities. The most widely used principles today are called *density porosity* and *neutron porosity*. These are investigated in detail here, the reader should refer to Smithson (2012) for a detailed explanation. Figure 2.4 illustrates the porosity property.

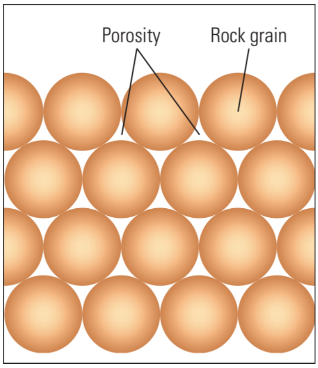

Figure 2.4: Porosity is determined by the pore and grain size distribution (Smithson, 2012)

2.3.2 Permeability

Permeability is the ability of a porous material to transmit fluid, i.e., the ease of which fluid can pass through it. Permeability is usually denoted the letter K, and is measured as the area of open pore space in the cross section that faces, or is perpendicular to, the direction of flow (Nolen-Hoeksema, 2014). Hence, its SI unit of measurement is m^2. However, it is more common to use the *darcy* unit (1 D $\approx 1 \cdot 0.987^{-12}$ m^2), named after the French scientist Henry Darcy. It is normal that the permeability varies widely within a reservoir, and ranges from 1 mD to 10 D are not unusual. Permeability appears in Darcy's law, which describes the steady-state flow of single-phase fluid through porous media (Lie and Mallison, 2013):

$$\vec{v} = -\frac{K}{\mu}\nabla\Phi \tag{2.4}$$

where $\vec{v}$ is the superficial velocity, μ is the viscosity, ρ is the density and $\nabla\Phi$ is the pressure gradient (i.e. $\nabla\Phi = \nabla p - \rho||\vec{g}||z$, where $||\vec{g}||$ is the gravity constant and z is the height value). Permeability is closely related to porosity, and high porosity often implies high permeability. However, this is not always the case, as high permeability is also a matter of *connectivity*, i.e., how well the pores are connected to each other enabling fluid to flow in between. Assuming laminar (streamline) flow, permeability and porosity is related through the Carman-Kozeny equation

$$K = \frac{1}{8\tau A_v^2}\frac{\phi^3}{(1-\phi)^2} \tag{2.5}$$

where τ is the tortuosity, meaning the ratio between the actual distance traveled and the straight-line distance (also called arc-chord ratio) and A_v is the specific surface area (internal surface per unit bulk volume). It is important to emphasize that permeability is a scalar only in the case of an *isotropic* (as opposed to anisotropic) medium. In general, fluid will flow easier in one direction through a material than another, meaning a tensor is required to fully describe the permeability. Also, permeability as described in this section is actually called *absolute* permeability. In the context of multi-phase flow, it is important to separate between absolute permeability and *relative* permeability (see Section 2.5.1). Figure 2.5 displays the principle of permeability.

2.3.3 Hydrocarbon saturation

The hydrocarbon saturation is a property that renders how much of a porous rock that is occupied by hydrocarbons, i.e. the fraction of the rock filled with oil or gas. Thus, the saturation is a dimensionless number in the range $[0, 1]$, just like porosity. The equation describing saturation uses the fact that as water in a porous rock is displaced by oil, the conductivity in the rock decreases. This

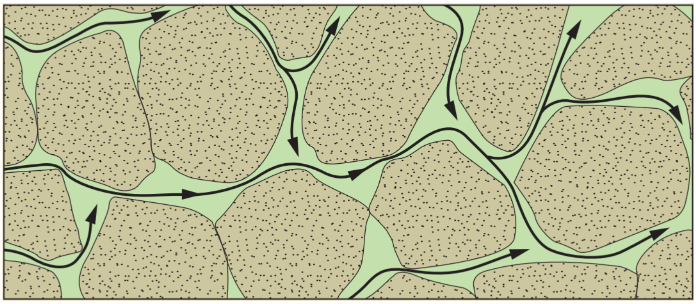

Figure 2.5: Permeability is the ability for fluid to flow through a porous material (Nolen-Hoeksema, 2014)

relationship is displayed in Eq. (2.6), which is called Archie's Law:

$$C_t = S_w^n \phi^m C_w \tag{2.6}$$

where C_t is the conductivity of the oil-bearing rock sample, S_w is the water saturation, ϕ is the porosity and C_w is the pore water conductivity. The saturation exponent, n, expresses the increased difficulty for an electrical current to pass through the rock sample as it becomes *desaturated*, i.e. as the water is replaced by non-conductive oil. A typical value is $n = 2$.[1] The cementation exponent, m, expresses how the connectivity of the pore structure affects the conductivity, as the rock itself is assumed to not conduct electricity. A common value is $m = 2$.[1] Most logging tools measure resistivity, the reciprocal of conductivity, hence Equation (2.6) is usually inverted to (Frank Jahn, Mark Cook, 2008)

$$R_t = S_w^{-n} \phi^{-m} R_w \tag{2.7}$$

where R_t and R_w is the formation and water resistivity, respectively. The water saturation is easily extracted as

[1] Values are collected from the Schlumberger Oilfield Glossary, `http://www.glossary.oilfield.slb.com/`

$$S_w = \sqrt[n]{\frac{R_w}{\phi^m R_t}} \tag{2.8}$$

Since saturation is a fraction, the hydrocarbon saturation is obviously found as

$$S_h = 1 - S_w \tag{2.9}$$

2.4 Fluid properties

In order to model fluid flow in a reservoir, it is not enough to have knowledge of the reservoir rocks. The flow is also highly dependent fluid characteristics, thus these are also important to obtain.

2.4.1 Viscosity

Viscosity is a measure of a fluid's resistance to shear stress, although commonly referred to as "thickness". High viscosity indicates a thick (viscous) fluid, such as oil, while low viscosity indicates a thin fluid, such as air. Viscosity is usually derived through the so-called moving plate model. Consider a plate sliding on the floor, with fluid underneath. When the plate moves, the fluid is subject to a shear stress defined by

$$\tau = \frac{F}{A} \tag{2.10}$$

where F is the horizontal component of the force used to move the plate and A is the plate's area. The shear stress creates a velocity profile where the fluid has the same velocity as the plate on top, denoted u, and zero velocity at the bottom (see Figure 2.6). This is called the *no-slip condition.* Sir Isaac Newton postulated in 1687 a differential equation relating the shear stress τ to the fluid velocity gradient (White, 2003)

$$\tau = \mu \frac{\mathrm{d}u}{\mathrm{d}y} \tag{2.11}$$

where y is the vertical distance away from the floor. The proportionality constant is the fluid's viscosity, also referred to as the *dynamic viscosity*. The viscosity of a given fluid varies highly with temperature and slightly with pressure.

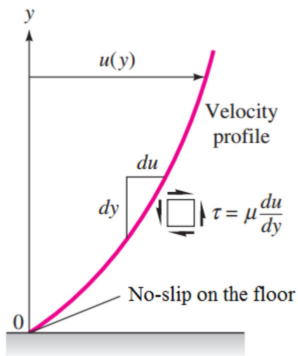

Figure 2.6: The velocity profile in the fluid as the plate moves with velocity u (adapted from White (2003))

2.4.2 Relative permeability

When several phases (e.g. oil, gas, water) are present in a fluid, this usually inhibits flow. Thus, when considering multi-phase flow, the permeability (absolute permeability) property must be extended to be phase dependent. This is done by introducing the *relative permeability*, usually denoted $k_{r\alpha}$, of phase α. The relative permeability is a dimensionless number in the interval $[0,1]$ that reflects the proportion of the absolute permeability of that phase at total saturation (i.e. if it was the only phase present) that is effective in the fluid. The product of the relative permeability and the absolute permeability is called the *effective permeability*, denoted k_α, thus the following relationship is applicable:

$$k_{r\alpha} = \frac{k_\alpha}{K} \tag{2.12}$$

A single-phase fluid has relative permeability equal to 1. However, in a multiphase, the sum of the relative permeabilities is less than unity because of intermolecular forces between the phases present. That is, for an oil-water-gas system, for instance, then

$$k_{ro} + k_{rw} + k_{rg} < 1 \tag{2.13}$$

Relative permeability is usually regarded as a function of saturation only, and some approximative models that relate these two properties exist. Nonetheless, relative permeability is usually obtained by performing laboratory experiments on core samples from the reservoir (Frank Jahn, Mark Cook, 2008). Figure 2.7 shows a typical diagram for the relative permeabilities in a fluid consisting of oil and gas. S_{or} is the residual oil saturation, i.e. the saturation at which no more oil can be recovered. S_{gc} is the critical gas saturation, i.e. the saturation at which the gas becomes mobile, hence able to flow.

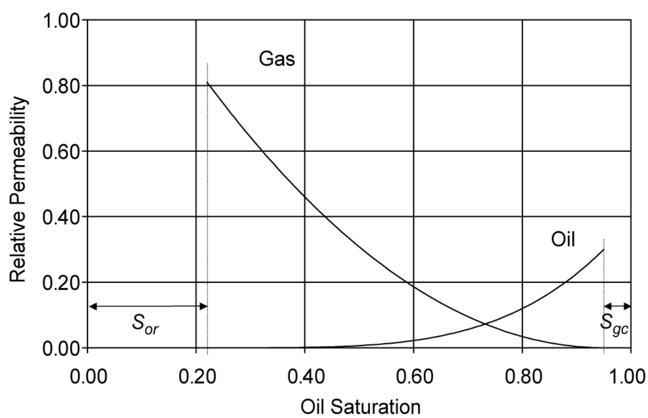

Figure 2.7: Relative permeability curve for oil and gas (www.petrowiki.org)

2.5 Modeling flow in porous media

Sections 2.3 and 2.4 cover the most central rock and fluid properties in reservoir modeling. These properties are important for understanding the differential equations used to describe fluid flow in a reservoir. While there is a lot of material available in the literature, this section covers the most widely used flow models in reservoir simulation. For a comprehensive review the reader is encouraged to consult Chen et al. (2006).

2.5.1 Two-phase flow

There are many ways to describe the flow of fluids in porous media, and it is all about making assumptions that are reasonable to the problem at hand to limit the complexity in the equations. This work focuses mainly on two-phase flow, where the fluid is assumed to be comprised of two immiscible phases, typically oil and water. The immiscible property means that the different phases don't mix together and form a solution. Recall that Equation (2.9) assumes immiscibility. Water is often referred to as the *wetting phase* and oil as the *non-wetting phase* (Chen et al., 2006). Recalling Darcy's law for single-phase flow (2.4), the two-phase extension is easily derived as (Lie and Mallison, 2013)

$$\vec{v}_\alpha = -\frac{k_{r\alpha} K}{\mu_\alpha} \nabla \Phi_\alpha \tag{2.14}$$

where $\alpha \in \{o, w\}$ is the phase indicator and $k_{r\alpha}$ is the relative permeability for phase α. Notice that the relative permeability is used as a scaling factor for the absolute permeability. Moreover, the principle of mass conservation applies to each phase, i.e.,

$$\frac{\partial(\rho_\alpha S_\alpha \phi)}{\partial t} = -\nabla \rho_\alpha \vec{v}_\alpha + q_\alpha \tag{2.15}$$

where q_α is the mass flow rate of phase α per unit volume. Equations (2.14) and (2.15) together with the saturation equation (2.9) and the principle of capillary pressure, i.e.

$$p_c = p_o - p_w \tag{2.16}$$

is what constitutes the model for two-phase immiscible flow through porous media (Codas et al. (2015), Chen et al. (2006)). Furthermore, ϕ_α and μ_α are assumed to be functions of p_o, whereas $k_{r\alpha}$ and p_c are functions of S_w. The solution of a reservoir simulation are thus p_o and S_w as functions of space and time, given initial conditions $p_o(t_0)$ and $S_w(t_0)$, and boundary conditions as constraints on q_α and the corresponding well equations (Codas et al., 2015). There are several ways to rewrite the system (2.9, 2.14-2.16), see Section 2.3.2 in Chen et al. (2006). A common reformulation is to have a flow equation for fluid pressure and transport equations for saturations (Lie and Mallison, 2013).

2.5.2 Discretization and numerical solution

In order for the reservoir simulator to solve the flow equations across the model's grid structure, the system (2.9, 2.14-2.16) must be discretized in time and space. There are several ways to do this, the two most widely used being *finite differences methods* and *finite element methods* (Chen et al., 2006). Codas et al. (2015) contains a full discretization, including well models, where the Control Volume Finite Element Method is used for the space discretization and a Backward Euler Implicit Integration approach for the time discretization. Before the equations are stated, some new notation must be introduced. Let $B_\alpha = V_\alpha / V_{\alpha s}$ be the volume formation factor for phase α, where V_α and $V_{\alpha s}$ are the fluid bulk volumes at reservoir and stock tank conditions, respectively. Moreover, let $\lambda_\alpha = \frac{k_{r\alpha}}{\mu_\alpha B_\alpha}$ be the fluid mobility. The discretized system can be written (Codas et al. (2015), notation slightly adapted)

$$0 = \frac{1}{t_k - t_{k-1}} \left(\left[\frac{\phi^i S^i_\alpha}{B^i_\alpha} \right]_k - \left[\frac{\phi^i S^i_\alpha}{B^i_\alpha} \right]_{k-1} \right) - \left[\sum_{j \in N(\Omega_i)} \lambda^{i,j}_\alpha T^{i,j} \left(\Phi^j_\alpha - \Phi^i_\alpha \right) + \frac{q^i_\alpha}{B^i_\alpha} \right]_k \tag{2.17}$$

$$0 = \frac{q^i_{\alpha,k}}{B^i_{\alpha,k}} - \left[\sum_{w \in \mathscr{W}^i} W^I_{w,i} \lambda^{w,i}_\alpha \left(p^w_{\text{bh}} - p^i_\alpha - \rho^i_\alpha ||\vec{g}|| \left(z^w_{\text{bh}} - z^i \right) \right) \right]_k \tag{2.18}$$

$$0 = 1 - \left[S^i_w + S^i_o \right]_k \tag{2.19}$$

$$0 = \left[p^i_c - p^i_o + p^i_w \right]_k \tag{2.20}$$

Some further explanation is needed to understand Equations (2.17)-(2.20). Let $\Omega = \{\Omega_i\}, i \in \mathscr{G}$ be the reservoir domain, where Ω_i is a grid block and $\mathscr{G}$ is the set containing all grid blocks comprising Ω. The set $N(\Omega_i)$ contains all neighboring grid blocks to Ω_i. Thus, the superscripts i and j are spatial indices, whereas the subscript k is the time step index. Moreover, $\lambda^{i,j}$ is called the upstream mobility, meaning $\lambda^{i,j} = \lambda^j$ if $\Phi^j_\alpha > \Phi^i_\alpha$ or otherwise $\lambda^{i,j} = \lambda^i$. $T^{i,j}$ is a constant. Equation (2.18) contains some new well variables, where the set $\mathscr{W}^i$ composes all wells perforating grid block Ω_i. $\lambda^{w,i}_\alpha$ is the upstream mobility of well perforation i and p^w_{bh} is the bottomhole pressure (BHP) in well w, measured at height z^w_{bh}. $W^I_{w,i}$ is a productivity constant. Equations (2.18)-(2.20) can be used to replace $p^i_{w,k}$, $S^i_{o,k}$ and $q^i_{\alpha,k}$ in Equation (2.17). At each time step, two equations with two reservoir variables ($p^i_{o,k}$ and $S^i_{w,k}$) and $|\mathscr{W}|$ well variables must be solved for all grid blocks.

2.5.3 The black-oil model

The most widely used flow model in reservoir simulation is the black-oil model. This is a three-phase model, where the regular hydrocarbon phase is divided in two; oil and gas. At surface conditions these two are completely undissolved (separated), while at reservoir conditions the gas can be dissolved in the oil, partially or completely. The third phase is water, which is always undissolved from the hydrocarbon phases. Recalling the volume formation factors explained in Section 2.5.2 and introducing the *gas solubility factor* $R_{so} = V_{gs}/V_{os}$ (i.e. the volume of gas dissolved in the oil at reservoir conditions), the black-oil model equations are written (Lie and Mallison, 2013)

$$\frac{\partial}{\partial t}\left(\frac{\phi\rho_s^\alpha}{B_\alpha}S_l\right) + \nabla\cdot\left(\frac{\rho_s^\alpha}{B_\alpha}\vec{v}_l\right) = q^\alpha, \ \alpha = o, w \tag{2.21}$$

$$\frac{\partial}{\partial t}\left(\frac{\phi\rho_s^g}{Bg}S_g + \frac{\phi R_{so}\rho_s^g}{B_o}S_l\right) + \nabla\cdot\left(\frac{\rho_s^g}{B_g}\vec{v}_g + \frac{R_{so}\rho_s^g}{B_o}\vec{v}_l\right) = q^g \tag{2.22}$$

which must be expressed for each fluid component l present. Most commercial reservoir simulators have solvers for black-oil equations.

2.6 Reservoir simulation software

There are several reservoir simulation softwares available on the market, both commercial and open-source. The most widely recognized is ECLIPSE from the oil field services company Schlumberger. It has been continuously developed in over 30 years and is considered by many to be the industry leader. ECLIPSE supports virtually all reservoir types, including unconventional fields (e.g. shale oil and gas), in addition to a multitude of options for Enhanced Oil Recovery (EOR) methods (e.g. gas injection) and field development strategies. Other commercial simulators are Nexus, owned by the oil field services company Halliburton, MoReS from Shell and the General Purpose Research Simulator (GPRS), developed at Stanford University.

2.6.1 Matlab Reservoir Simulation Toolbox

All simulations in this work are performed using the Matlab Reservoir Simulation Toolbox (MRST). This is a free open-source program developed by SINTEF Applied Mathematics and published in 2009 under the terms of the GNU General Public License. MRST has received increased attention since its release, mostly due to its low-threshold interface and relatively low requirements to processing capacity. MRST comprises mainly two parts; a core and a set of add-on modules. The core consists of basic routines for creating grids and assigning petrophysical properties, and contains solvers for incompressible, immiscible and simple single-phase and two-phase flow equations. The add-on modules are extensions of the core with more advanced functionality, typically solvers to more complex models (e.g. black-oil) as well as support for other reservoir model formats, e.g. ECLIPSE. For a complete list of available add-on functionality, consult section 1.4 in Lie (2014). Figure 2.8 displays the structure of MRST.

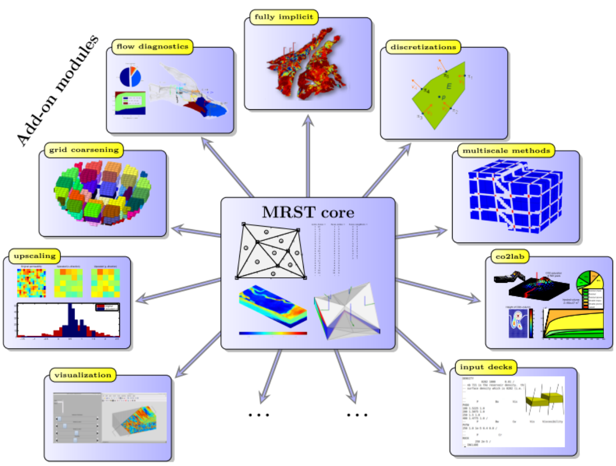

Figure 2.8: Structure of MRST (Krogstad et al., 2015)

Chapter 3

Reservoir Management under Uncertainty

Uncertainty poses a big challenge in oil and gas production. Despite very accurate measuring tools, highly advanced modeling software and the best professional expertise, it is quite obvious that obtaining a correct description of a subsurface reservoir is impossible. This means that the information that engineers and geoscientists use to plan and execute the production is uncertain, i.e., it is not necessarily correct. This chapter addresses the uncertainty problem in reservoir management. The goal is to give the reader an overlying understanding of where the uncertainties come from, how they are identified and visualized, and last but not least, methods for handling the uncertainties. First, the reader is introduced to the concept of reservoir management, and its strong relation to production optimization. The optimal control problem for reservoir optimization is formulated and explained. In Section 3.3 the reader is introduced to how uncertainty can be included in optimization problems, and how they can be solved using stochastic programming. The methods discussed have existed for quite a while, but have seen limited use in oil and gas production.

3.1 Reservoir Management

Reservoir management is a very important area of oil and gas production. It is an extensive topic that has received a lot of research attention for many decades, thus there is very much material available in the literature. While there are many different explanations accessible, they all have a lot in common, and the following definition seeks to capture the most important purpose.

Definition. *Reservoir management is the flow of multi-disciplinary decisions regarding the operation of an oil field's production facilities, with the purpose of maximizing hydrocarbon recovery.*

To better understand what kind of decisions reservoir management involves, the reader should be familiar with the bigger picture of hydrocarbon production systems. While it is desirable to control all parts of the system simultaneously, this has not yet been possible to achieve due to size and complexity challenges. However, the various parts of most oil and gas systems have big differences in time constants. For example, a reservoir has much slower dynamics than the wells used to extract the oil. This makes it reasonable to divide the control system into several layers, and place them in a hierarchical manner. Figure 3.1 displays the four levels in process control systems, with typical decisions and corresponding time scales listed on the sides of each level. Ideally, there are bidirectional connections between all levels. The bottom level is called Control and Automation and is where the classical controllers (e.g. Proportional-Integral-Derivative controllers (PID)) are found, in addition to more advanced Model Predictive Control (MPC) algorithms. Above Control and Automation there is Production Optimization, which will be further discussed in Section 3.2. This level constitutes what is called *short term optimization*, and involves decisions such as deciding injection rates and routing well streams between pipelines (Foss, 2012). In the literature, these decisions are sometimes included in the reservoir management domain, thus there is a strong coupling and a blurry border between these two levels. As seen, Reservoir Management decisions typically lie in the time scale of months. This includes planning wells (type, location etc.), supporting drilling operations and executing recompletions, to name a few. The top level is Asset Management, and covers the long term planning and strategy making. During exploration, this typically means planning and executing seismic surveys. When a discovery has been made, it involves developing a depletion plan for the reservoir and choosing a suitable Enhanced Oil Recovery technique, if needed. Moreover, Asset Management also covers investment strategies, transportation and export, and legal relationships. Note that there are other classifications of the process control hierarchy available in the literature, e.g. in Seborg et al. (2011).

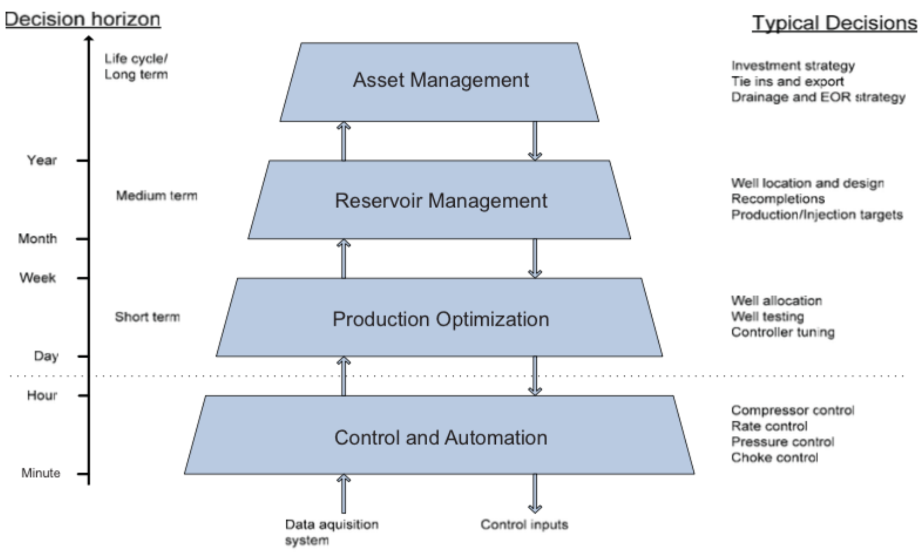

Figure 3.1: The process control hierarchy (Foss and Jensen, 2011)

3.2 Production optimization

Production optimization is concerned with how to use the existing production facilities to ensure maximal recovery. That is, given a certain configuration of production equipment (injectors and producers with fixed locations), how should these be tuned to maximize oil production?

3.2.1 Producing an oil field

According to Van Essen et al. (2010), there are two main stages in the production phase. In the first stage, it is the reservoir pressure itself that acts as the main driving force for the well flows. The clue is that the bottomhole pressure in the production wells must be lower than the reservoir pressure in order to make oil flow into the wells, and it is the magnitude of this pressure difference that determines the flow rates. As the reservoir is drained, the pressure drops, and hence this difference decreases. To sustain the reservoir pressure, fluid is injected via dedicated injection wells. The injected fluid, usually water, is also meant to "push" the remaining oil in the reservoir towards the producers, which is called *sweeping* the reservoir. This technique is referred to as waterflooding. Eventually the water front itself will reach the producers, recognized as the wells producing less oil and noticeably more water. This is called the water-breakthrough. It is obviously desirable to delay the water-breakthrough as much as possible, and this is perhaps the main purpose of production optimization. Figure 3.2 illustrates the principle of waterflooding on a simplified reservoir with two horizontal wells (one injector and one producer). As seen, the water front does not move uniformly towards the producer. This is because of heterogeneity in the rock permeability, i.e., fluids flow easier some places than others. Notice the water-breakthrough on the picture to the right.

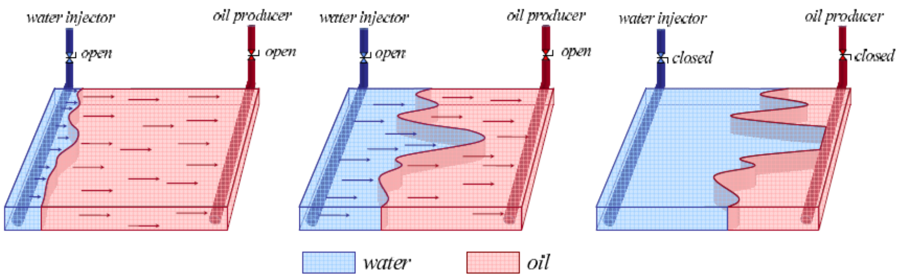

Figure 3.2: The waterflooding principle (Van Essen et al., 2010)

3.2.2 A reactive production strategy

Figure 3.2 illustrates a common production strategy, where the producer is kept open until the water-breakthrough occurs, at which it is shut in. This is called a *reactive* approach. The water-breakthrough is usually recognized as a predefined water-cut ratio, typically 80-90 %. This value indicates when it is no longer profitable to produce from the well in question, thus it varies from well to well and reservoir to reservoir. For example, several wells on the Brage field in the North Sea produces more than 90 % water and consequently less than 10 % oil. The reactive production approach has the advantage of not requiring a reservoir model, but often suffers from leading to non-optimal oil recovery. Figure 3.2 exemplifies this by showing that after the wells are shut in, there are still significant amounts of oil left in the reservoir.

3.2.3 Model based production optimization

This work focuses on model based production optimization, i.e., formulating the problem as a mathematical optimization problem. This section uses the problem setup in Codas et al. (2015), with a slight simplification. Let $\mathcal{K} = \{1,...,K\}$ be the prediction horizon with K time steps, and $\mathcal{U} = \{1,...,U\}$ the control horizon with U steps. Moreover, define the state vector $x = \{x_k\} = \{p^i_{o,k}, S^i_{w,k}\}, k \in$

$\mathcal{K}, i \in \mathcal{G}$ and the control vector $u = \{u_j\}, j \in \mathcal{U}$. That is, the states are oil pressure and water saturation for all grid cells $\Omega_i, i \in \mathcal{G}$, where $\mathcal{G}$ is the set containing all grid cells comprising the reservoir domain Ω. The control variables are typically fixed bottom hole pressures or output flow rates on the wells, or a combination of the two. For each time step $k \in \mathcal{K}$, there is a surjective function $\kappa(k)$ mapping the time step to the correct control step, as there can be fewer control steps than time steps. Furthermore, define the vector $v = \{q^w_{\alpha,k}, p^w_{\text{bh},k}\}, k \in \mathcal{K}, w \in \mathcal{W}, \alpha \in \{o, w\}$ of well variables, where $\mathcal{W}$ is the set of wells. Given initial condition x_0, the optimal control problem is formulated as

$$\min_{u \in \mathbb{R}^{|\mathcal{W}|}} \quad \sum_{k \in \mathcal{K}} J_k(v_k, u_{\kappa(k)}) \tag{3.1a}$$

$$\text{subject to} \quad x_{k+1} = R^x(x_k, u_{\kappa(k)}), k \in \mathcal{K} \tag{3.1b}$$

$$v_k = R^v(x_k, u_{\kappa(k)}), k \in \mathcal{K} \tag{3.1c}$$

$$b^x_l \leq x_k \leq b^x_u, k \in \mathcal{K} \tag{3.1d}$$

$$b^v_l \leq v_k \leq b^v_u, k \in \mathcal{K} \tag{3.1e}$$

$$b^u_l \leq u_{\kappa(k)} \leq b^u_u, k \in \mathcal{K} \tag{3.1f}$$

The reservoir functions $R^x(x_k, u_{\kappa(k)})$ and $R^v(x_k, u_{\kappa(k)})$ are equivalent to the system (2.17)-(2.20). $R^v(x_k, u_{\kappa(k)})$ also includes one equality constraint for each well, relating v_k to the corresponding control target $u_{\kappa(k)}$. Equations (3.1d)-(3.1e) are called output constraints, whereas Eq. (3.1f) obviously is the input constraint. For a well controlled by bottomhole pressure, the output constraint is typically a limit on the flow, and vice versa. The objective function $J_k(v_k, u_{\kappa(k)})$ can be any optimization target, e.g. Net Present Value (NPV) or cumulative oil production (in which cases (3.1) becomes a maximization problem). A common way to calculate NPV is (Lorentzen et al., 2009)

$$\text{NPV} = \sum_{k \in \mathcal{K}} \Delta t \frac{q_o r_o - q_w r_w - q_i r_i}{(1 + b/100)^{t_k}} \tag{3.2}$$

where Δt is the size of each time step (usually number of days), q_o is the oil production rate (usually Sm^3/day or STB/day), r_o is the oil price (usually USD/Sm^3 or USD/STB), q_w is the water production rate, r_w is the cost of producing water, Q_i is the injection rate, r_i is the injection cost, b is the discount rate and t_k is the elapsed time.

3.2.4 Solution of reservoir control optimization problems

In general, performing a full reservoir simulation over the whole prediction horizon is a computationally intensive task. Thus, solving reservoir optimal control problems is even more demanding, as optimization algorithms require many simulations in order to find an optimal solution. In so-called direct methods, the optimal control problem (3.1) is transformed into a Nonlinear Programming (NLP) problem (Codas et al., 2015). The NLP problem is usually solved with a gradient-based algorithm, in which the optimal solution is found by searching along the ascending (or descending) direction of the objective function. For each iteration, the reservoir must be simulated for the current control guess to evaluate the output values, from which the algorithm computes the next step. This sequential procedure is called *Single Shooting* (SS).

Obtaining gradients

A gradient-based algorithm needs to evaluate the derivatives of the objective and constraint functions with respect to the control variables. The most common approach for obtaining the gradients is to solve a system of adjoint equations (see Jansen (2011) for a comprehensive overview). Usually, obtaining the gradient of the objective function, as well as simple bounds on the control input, is an easy linear operation. However, output constraints pose an issue as they are often nonlinear functions of the current simulation result. That is, they depend not only on the control inputs, but also on the state variables. Limits on the oil production rate for a single well or the total water production rate for a group of wells are examples of nonlinear output constraints (Codas et al., 2015). In a Single Shooting setting, each output constraint require one additional adjoint computation (Codas et al., 2015). A possible way to overcome this is to lump the constraints into one, but this also introduces new infeasibility issues.

REMSO

REMSO is an optimization algorithm for MRST developed by PhD student Andres Codas at the Norwegian University of Science and Technology. It is an abbreviation for Reservoir/Reduced Multiple Shooting Optimization, and can be used to solve optimal control problems for oil and gas applications. REMSO uses a *Multiple Shooting* (MS) strategy, which is an alternative to Single Shooting that deals with the main drawbacks. In MS, the prediction horizon is divided into several intervals, each of which is solved as an independent initial value problem (IVP). The advantage is that the state variables are explicitly available at certain points in the prediction horizon (namely as the initial conditions for each interval), which makes the output constraints become simple bounds. As the intervals are independent, they can be simulated in parallel, utilizing multicore computer processors. The challenge of Multiple Shooting is to match the separate IVP solutions to form a single feasible optimal solution. Figure 3.3 illustrates the difference between the two methods. The REMSO optimization package also offers functionality to solve optimization problems with Single Shooting. The software is published under the GNU General Public License [1].

[1] Download is available from https://github.com/iocenter/remso

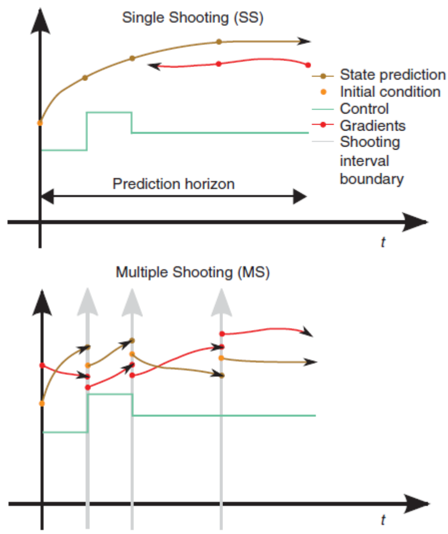

Figure 3.3: Single Shooting vs Multiple Shooting (Codas et al., 2015)

3.3 Optimization under uncertainty

As mentioned earlier, huge uncertainties accompany the reservoir model used in the optimal control problem. Even though today's measuring tools are very accurate, the main problem is that it is impossible to achieve measurements from every cubic centimeter of a reservoir that is located thousands of meters below the sea floor with lateral extension of several kilometers. This means that local measurements must be extended through the reservoir volume, which obviously introduces a lot of uncertainty. Also, even though measuring instruments provide accurate data, there is always error that contributes to the total model uncertainty.

The optimal control problem (3.1) is based on an uncertain reservoir model. This means that the optimal control law obtained when solving the problem might not give the predicted production scheme at all. One can say that it lacks *robustness* to geological uncertainty. Now, let's look at how uncertainty can be explicitly accounted for in optimization, and how this can make the solution robust.

3.3.1 Introducing uncertainty to the problem

Consider the following unconstrained optimization problem

$$\min_{u \in \mathbb{R}^n} J(u) \tag{3.3}$$

for some input $u \in \mathbb{R}^n$ and the objective $J(u)$ being the cumulative Net Present Value, negated so that (3.3) can be formulated as a minimization problem. The problem (3.3) is purely deterministic, meaning that J has a real numbered value for any given u. Now, say that the objective is also dependent on a vector of uncertain parameters $\xi \in \mathbb{R}^m$.[2] In an oil and gas application this could be rock properties, e.g. permeability or porosity, or an economic measure, e.g. oil price. The problem is now

$$\min_{u \in \mathbb{R}^n} J(u, \xi) \tag{3.4}$$

Since ξ is a stochastic variable, it can take any value within the so-called *uncertainty set* $\Xi \subset \mathbb{R}^m$ (also called the *support* of the random variable). This means that the objective is no longer uniquely determined for a given u, i.e., instead of mapping to a real numbered NPV, it maps to an NPV *distribution.* The input u is called a decision, and different decisions will typically give different distributions, as illustrated on Figure 3.4.

Stochastic variables require different treatment than real variables, thus the stochastic problem (3.4) cannot be solved with the same algorithms as the deterministic problem (3.3). A common way to overcome this is to use the expected values of

[2] This work considers real-valued stochastic variables. In general, ξ can be complex.

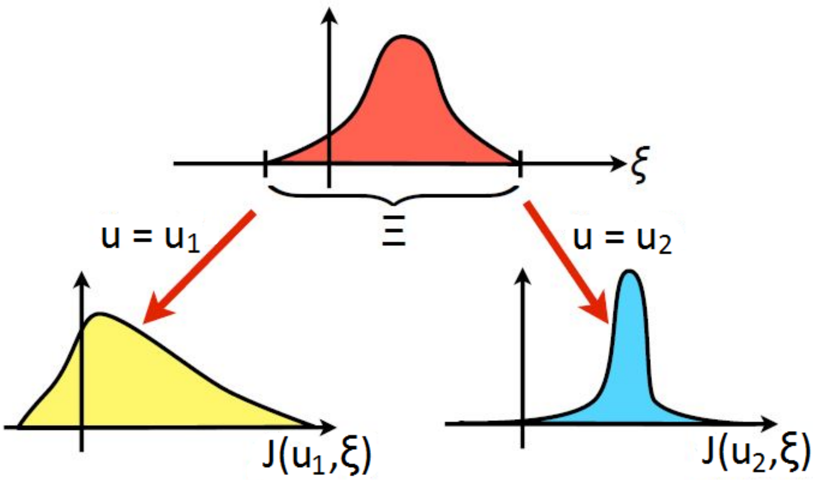

Figure 3.4: Different decisions lead to different distributions of the objective (adapted from Daniel Kuhn, EPFL)

the uncertain parameters, and thereby transform the stochastic problem to a deterministic problem where the conventional methods apply. That is, to solve the problem

$$\min_{u \in \mathbb{R}^n} J\big(u, \mathbb{E}[\xi]\big) \tag{3.5}$$

However, this approach basically ignores the uncertainty. The solution of (3.5) tells us how the NPV can be maximized given that the uncertain parameters are what we *think* they are. It does not say anything about how the solution will work if they are not. If the variance of ξ is large, then the solution of (3.5), which is referred to as the deterministic solution, is almost guaranteed to be misguiding. Thus, the uncertainty should be treated in a better way. According to Van Essen et al. (2009) there are two ways to deal with uncertainty in modeling and control: reducing the uncertainty itself or reducing the *sensitivity* to the uncertainty. The most widely used method to reduce uncertainty in a reservoir model is called history matching, and is briefly discussed in Section 3.3.2. When talking about reducing the sensitivity to uncertainty, it means handling the uncertain parameters explicitly in the optimization. The framework that covers this is called stochastic programming, and is the topic of Section 3.3.3.

3.3.2 History matching

History matching has become a widely used methodology for reducing uncertainty in a reservoir model. Briefly explained, history matching is the act of iteratively adjusting the parameters in a reservoir model to reproduce known production data. One usually distinguishes between manual and automatic history matching. The manual approach is when an engineer or geoscientist adjust the parameters based on knowledge and experience. This can work very well for smaller problems where the number of parameters to adjust is manageable, but for large-scale reservoir models it is unrealistic. Automatic history matching is based on general parameter estimation techniques, where an objective function to be minimized is formulated, usually as an error term between reference (production data) and measurement (model output), e.g. least squares. It is beyond the scope of this thesis to go into further details on parameter estimation methods. The reader is referred to Ioannou et al. (1996) for a full overview.

Closed-Loop Reservoir Management

The combination of automatic history matching and dynamic optimization has received increased attention over the last decade, usually under the name *Closed-Loop Reservoir Management* (CLRM). With CLRM, the reservoir model is updated before it is passed to the optimizer, and this is done repetitively at a frequency that fits the purpose of the model (i.e. it can be both short-term and long-term). Several research articles discuss this implementation of reservoir management, see e.g. Foss and Jensen (2011), Lorentzen et al. (2009) and Brouwer and Naevdal (2004). Figure 3.5 illustrates two possible implementations of CLRM.

Option (a) uses history matching to update the model once every year, with several input calculations (optimization steps) in between update. Option (b) updates the model for every input step.

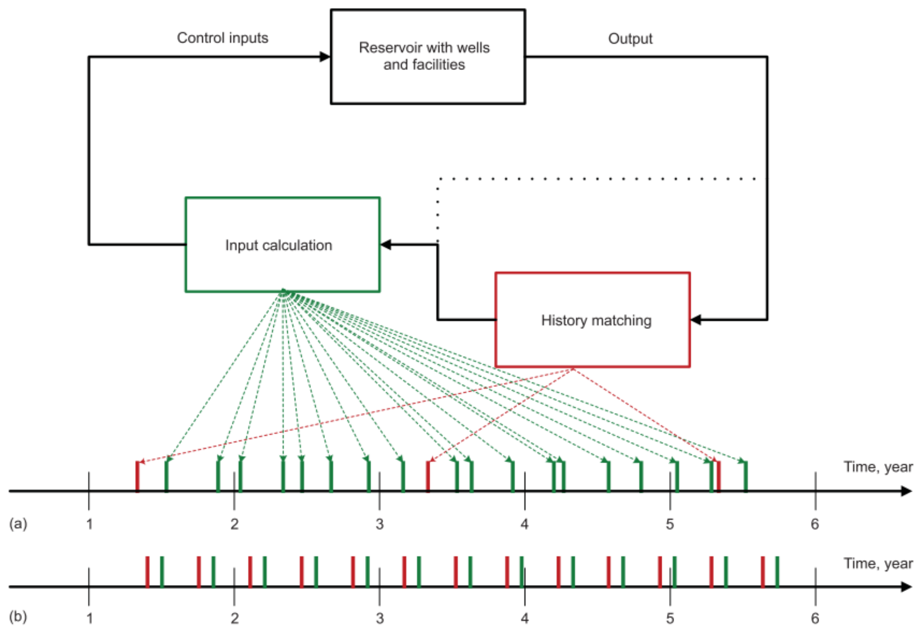

Figure 3.5: Closed-Loop Reservoir Management (Foss and Jensen, 2011)

3.3.3 Stochastic programming

The solution to the deterministic problem (3.5) maximizes NPV when the uncertain parameters are equal to their expected values. As already mentioned, this does not provide useful insight to the problem. Consider instead the following formulation,

$$\min_{u \in \mathbb{R}^n} \mathbb{E}\big[J(u,\xi)\big] \tag{3.6}$$

i.e., to maximize the *expected* NPV over the uncertainty space spanned by ξ. Note the difference from Eq. (3.5), as

$$\mathbb{E}[J(u,\xi)] \neq J(u,\mathbb{E}[\xi]) \tag{3.7}$$

in general. The expected value operator in Eq. (3.6) is called a *decision criterion*, as it reflects what the decision maker considers to be a desired property of the objective distribution. The expected value is the most widely used decision criterion in stochastic programming applications, for a good reason. In applications where the decision is repeated many times, the Law of Large Numbers guarantees that the observed outcome average will tend to the expected value. Hence, in such cases it makes sense to optimize the expected value and not care so much about individual variations. Generally in applications where the decision maker does not have to be risk averse, the expected value approach is a good way of handling uncertainties. In general, it can be replaced with any statistical measure, some of which are listed in Table 3.1.

Table 3.1: Popular decision criteria

Name	**Minimization problem formulation**[3]
Variance	$\min_{u\in\mathbb{R}^n} \text{Var}[J]$
Mean-Variance Functional	$\min_{u\in\mathbb{R}^n} \lambda\mathbb{E}[J] + (1-\lambda)\text{Var}[J]$
Value-at-Risk	$\min_{u\in\mathbb{R}^n} \text{VaR}_\eta[J] = \min_{\gamma} \{\gamma : \text{Prob}(J \leq \gamma) \geq \eta\}$
Conditional Value-at-Risk	$\min_{u\in\mathbb{R}^n} \text{CVaR}_\eta[J] = \mathbb{E}[J \mid J \geq \text{VaR}_\eta[J]]$
Worst case	$\min_{u\in\mathbb{R}^n} \sup_{\xi\in\Xi} [J]$

This work uses the expected value as the optimization target in the examples. For more details on each of the listed decision criteria, consult Midttun (2014). Some further explanation is given in Section 3.5.

[3]The objective function $J(u,\xi)$, here referred to as J for simplicity, is here a cost or a loss

3.4 Solution of stochastic optimization problems

The obvious question after introducing the concept of optimization under uncertainty is how such problems can be solved. That is, how to solve Eq. (3.6). The main concern is what to do with the expected value term. For simple problems, it might be possible to find the solution analytically. If this is not possible, which is the case in almost all reservoir applications, then it must be approximated. This section addresses the most widely used approximation technique in reservoir management.

3.4.1 The realizations ensemble

From a reservoir management perspective, uncertainty means that there are an infinite amount of models that could fit the measurement data available. To make this manageable, the standard approach is to discretize the uncertainty set Ξ. That is, the uncertain reservoir is modeled as a finite set of possible realizations, or scenarios. This set is often called the *realizations ensemble*. The realizations ensemble can be generated in several ways depending on the information available. An experienced geologist can create the scenarios manually based on his knowledge of the reservoir in question. Another possibility is to create the ensemble using a computer program. Figure 3.6 displays nine realizations of a fictive reservoir's permeability field, randomly chosen from an ensemble of 100. Notice that the permeability varies quite a lot among them. However, it is clear that the highly permeable channels are vertically aligned, which is a useful observation.

Regardless of which method is used to generate the possible scenarios, it is impossible to tell which of the realizations that is the true model. In fact, none of them are actually true, but if previous production data is available or the geo-

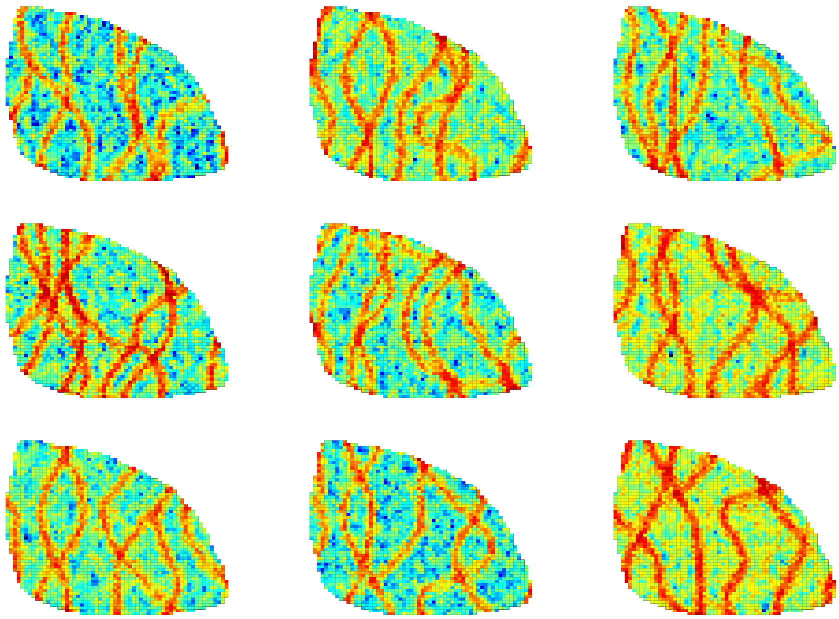

Figure 3.6: Nine realizations of a reservoir's permeability field

scientists have detailed knowledge of the reservoir, it might be possible to tell which of the realizations that are most likely to be close to the truth. This is called *ranking* the realizations (see Deutsch and Srinivasan (1996) or Ch. 4). Given a set of N_r realizations $\xi = \{\xi_1, \xi_2, ..., \xi_{N_r}\}$, the expected value term in Eq. (3.6) can be replaced with the sum of possible scenarios weighted by their respective probabilities. That is,

$$\mathbb{E}[J(u,\xi)] = \sum_{n=1}^{N_r} p_n J(u,\xi_n) \tag{3.8}$$

where $\sum_{n=1}^{N_r} p_n = 1$. This is called the *finite scenario approximation*. In the special case of equiprobable realizations, Eq. (3.8) becomes the *Sample Average Approximation* (SAA),

$$\mathbb{E}[J(u,\xi)] = \frac{1}{N_r} \sum_{n=1}^{N_r} J(u,\xi_n) \tag{3.9}$$

which is a Monte Carlo method. Equiprobable here means that the realizations $\xi_n,\ n = 1,...,N_r$ are independent identically distributed (IID).

Choice of sample size

Obviously, a finite set of scenarios will never render the truth completely. However, if the ensemble is big enough, it is a question of whether it is a *good enough* representation of the true reservoir. For the SAA approach, it is known from statistical theory that the expected variance of the sample average is inversely proportional to the number of samples. That is, for $\overline{J}_{N_r}(u,\xi) = \frac{1}{N_r}\sum_{n=1}^{N_r} J(u,\xi_n)$ then $\text{Var}\left[\overline{J}_{N_r}(u,\xi)\right] = \frac{1}{N_r}\text{Var}\left[J(u,\xi)\right]$. This means that the standard deviation decays by a factor of $\frac{1}{\sqrt{N_r}}$. Thus, for every 100 samples added the accuracy is improved by 0.1 (Shapiro and Philpott, 2007). In real applications, a set of 100 realizations is usually considered satisfactory (Van Essen et al., 2009).

3.5 Handling output constraints

When optimizing under uncertainty, output constraints pose an issue because the uncertainty makes it difficult to know whether they will actually be satisfied or not. A typical example in oil and gas production optimization is the water handling problem. A production system typically has an upper water processing capacity, meaning the total rate of water coming from the producers must obey this constraint. If the producers are controlled by bottomhole pressure, for instance, uncertainty makes it hard to accurately predict what the actual output water rate will be. Thus, output constraints must be treated with care. Stochastic programming allows for handling output constraints in the same way as the objective function, i.e., using statistical measures as listed in Table 3.1. Let us look closer into what this involves.

3.5.1 The robust solution

When optimizing on a finite set of reservoir realizations, a possible approach is to require the output constraints to be satisfied for all realizations. This is called *robust* or *worst case* constraint handling. Formulating the ensemble optimization problem with robust constraint handling is straight forward. Consider the following set of equations, where the SAA approximation is used for the objective function:

$$\min_{u\in\mathbb{R}^{|\mathscr{W}|}} \quad \frac{1}{N_r}\sum_{n=1}^{N_r}\sum_{k\in\mathscr{K}} J_k(v_{k,n}, u_{\kappa(k)}) \tag{3.10a}$$

$$\text{subject to} \quad x_{k+1,n} = R_n^x(x_{k,n}, u_{\kappa(k)}),\ k\in\mathscr{K},\ n = 1,\dots,N_r \tag{3.10b}$$

$$v_{k,n} = R_n^v(x_{k,n}, u_{\kappa(k)}),\ k\in\mathscr{K},\ n = 1,\dots,N_r \tag{3.10c}$$

$$b_l^x \le x_{k,n} \le b_u^x,\ k\in\mathscr{K},\ n = 1,\dots,N_r \tag{3.10d}$$

$$b_l^v \le v_{k,n} \le b_u^v,\ k\in\mathscr{K},\ n = 1,\dots,N_r \tag{3.10e}$$

$$b_l^u \le u_{\kappa(k)} \le b_u^u,\ k\in\mathscr{K} \tag{3.10f}$$

The bound constraints on x and v must hold for all realizations $n = 1,\dots,N_r$. The robust solution makes sense to use in applications where constraint violations are critical, for example if they are directly related to safety. For the water handling problem, however, requiring the processing capacity to be satisfied for all realizations might result in an overly conservative solution, as any protruded scenarios will have large impacts on the solution. It is often desirable to be as close to the capacity limit as possible, and with the robust solution there is a chance that the actual response ends up too far away.

3.5.2 Chance constraints

An alternative to the robust formulation is to require the output constraints to be satisfied with a certain probability. In a general uncertain setting, given a constraint function $c(x,\xi)$, instead of requiring $c(x,\xi) \leq 0$ the *chance constraint* approach is to instead require

$$\text{Prob}(c(x,\xi) \leq 0) \geq \eta \tag{3.11}$$

where η is typically 90-95 %. Chance constraints can be expressed using the Value-at-Risk (cf. Table 3.1), as Eq. (3.11) is equivalent to

$$\text{VaR}_\eta(c(x,\xi)) \leq 0 \tag{3.12}$$

The Value-at-Risk is a measure that is used a lot in the financial sector, for example when optimizing a portfolio of stocks. Explained with words, the VaR at level $\eta \in [0,1]$ is a measure of the value for which the probability that the target will be less than or equal to this value is greater than or equal to η [4]. Figure 3.7 illustrates the VaR principle.

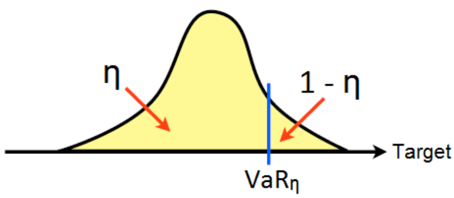

Figure 3.7: The Value-at-Risk (adapted from Daniel Kuhn, EPFL)

For the chance constraint formulation (3.12), the Value-at-Risk is only a measure of how certain a decision maker can be of not violating the constraint. It does not say what happens if the constraint actually ends up with being breached.

[4]The notation for the confidence level, here η, varies slightly in the literature

Hanssen et al. (2014) recommend using the expansion of Value-at-Risk, namely the Conditional Value-at-Risk (CVaR), to deal with this. The CVaR at level $\eta \in [0,1]$ is defined as the conditional expectation of the target above the corresponding VaR. That is, in the current context, the expected value of the constraint function, given that it is violated. With the CVaR formulation, the decision maker has an idea of what to expect if the constraint ends up being violated. We say that the CVaR regards the *tail* of the distribution. Cf. Table 3.1, the CVaR is expressed

$$\mathrm{CVaR}_\eta(c(x,\xi)) = \mathbb{E}[c(x,\xi) | c(x,\xi) \geq \mathrm{VaR}_\eta(c(x,\xi))] \tag{3.13}$$

The general and more rigorous definition is

$$\mathrm{CVaR}_\eta(c(x,\xi)) = \inf_{\beta \in \mathbb{R}} \left\{ \beta + \frac{1}{1-\eta} \mathbb{E}\left[\max\left(c(x,\xi) - \beta, 0 \right) \right] \right\} \tag{3.14}$$

Figure 3.8 illustrates the CVaR's position relative to the VaR. Furthermore, the CVaR is easily discretized over the realizations ensemble via the Sample Average Approximation (Hanssen et al., 2014):

$$\mathrm{CVaR}_\eta(c(x,\xi)) = \beta + \frac{1}{N_r(1-\eta)} \sum_{n=1}^{N_r} \left[\max\left(c(x,\xi_n) - \beta, 0 \right) \right] \tag{3.15}$$

where the max() expression can be replaced by introducing

$$z_n \geq c(x,\xi_n) - \beta \tag{3.16a}$$

$$z_n \geq 0 \tag{3.16b}$$

Using Equations (3.15)-(3.16), the ensemble optimization problem is formulated as

$$\min_{u\in\mathbb{R}^{|\mathcal{W}|}} \quad \frac{1}{N_r}\sum_{n=1}^{N_r}\sum_{k\in\mathcal{K}} J_k(v_{k,n}, u_{\kappa(k)}) \tag{3.17a}$$

$$\text{subject to} \quad x_{k+1,n} = R_n^x(x_{k,n}, u_{\kappa(k)}),\ k\in\mathcal{K},\ n=1,\dots,N_r \tag{3.17b}$$

$$v_{k,n} = R_n^v(x_{k,n}, u_{\kappa(k)}),\ k\in\mathcal{K},\ n=1,\dots,N_r \tag{3.17c}$$

$$\beta_u^x + \frac{1}{N_r(1-\eta)}\sum_{n=1}^{N_r} z_{u,n}^x \le 0,\ k\in\mathcal{K},\ n=1,\dots,N_r \tag{3.17d}$$

$$x_{k,n} - b_u^x - \beta_u^x \le z_{u,n}^x,\ k\in\mathcal{K},\ n=1,\dots,N_r \tag{3.17e}$$

$$z_{u,n}^x \ge 0,\ n=1,\dots,N_r \tag{3.17f}$$

$$\beta_l^x + \frac{1}{N_r(1-\eta)}\sum_{n=1}^{N_r} z_{l,n}^x \le 0,\ k\in\mathcal{K},\ n=1,\dots,N_r \tag{3.17g}$$

$$-x_{k,n} + b_l^x - \beta_l^x \le z_{l,n}^x,\ k\in\mathcal{K},\ n=1,\dots,N_r \tag{3.17h}$$

$$z_{l,n}^x \ge 0,\ n=1,\dots,N_r \tag{3.17i}$$

$$\beta_u^v + \frac{1}{N_r(1-\eta)}\sum_{n=1}^{N_r} z_{u,n}^v \le 0,\ k\in\mathcal{K},\ n=1,\dots,N_r \tag{3.17j}$$

$$v_{k,n} - b_u^v - \beta_u^v \le z_{u,n}^v,\ k\in\mathcal{K},\ n=1,\dots,N_r \tag{3.17k}$$

$$z_{u,n}^v \ge 0,\ n=1,\dots,N_r \tag{3.17l}$$

$$\beta_l^v + \frac{1}{N_r(1-\eta)}\sum_{n=1}^{N_r} z_{l,n}^v \le 0,\ k\in\mathcal{K},\ n=1,\dots,N_r \tag{3.17m}$$

$$-v_{k,n} + b_l^v - \beta_l^v \le z_{l,n}^v,\ k\in\mathcal{K},\ n=1,\dots,N_r \tag{3.17n}$$

$$z_{l,n}^v \ge 0,\ n=1,\dots,N_r \tag{3.17o}$$

$$b_l^u \le u_{\kappa(k)} \le b_u^u,\ k\in\mathcal{K} \tag{3.17p}$$

Notice that the lower and upper bounds on both x and v must be treated with separate CVaR formulations. That is, (3.17d)-(3.17f) represent the upper bound $c_u(x,\xi_n) = x_{k,n} - b_u^x \le 0$, whereas (3.17g)-(3.17i) represent the lower bound

$c_l(x, \xi_n) = -x_{k,n} + b_l^x \leq 0$. Correspondingly, (3.17j)-(3.17l) represent the upper bound $c_u(v, \xi_n) = v_{k,n} - b_u^v \leq 0$ and (3.17m)-(3.17o) represent the lower bound $c_l(v, \xi_n) = -v_{k,n} + b_l^v \leq 0$.

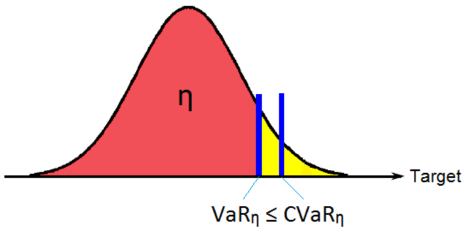

Figure 3.8: The Conditional Value-at-Risk (adapted from Daniel Kuhn, EPFL)

Convexity and coherence

For a linear function $c(x, \xi)$ and normally distributed ξ, the VaR constraint (3.12) becomes a second order cone constraint, i.e., a convex function. However, for non-linear functions it is non-convex. As shown in Shapiro and Philpott (2007), the CVaR is a convex approximation of the VaR. Unlike VaR, the CVaR also respects the subadditivity property, i.e., $\text{CVaR}(X+Y) \leq \text{CVaR}(X) + \text{CVaR}(Y)$. This makes the CVaR a *coherent* risk measure, as it satisfies the four axioms of translation invariance, subadditivity, positive homogeneity and monotonicity (Artzner et al., 1999). In the literature, the Conditional Value-at-Risk is sometimes referred to as the *expected shortfall* or *Average Value-at-Risk*.

Chapter 4

Literature Review: Reservoir Management under Uncertainty

This chapter contains a literature review of related work on reservoir management under uncertainty. A decent amount of research has been made to this topic, as uncertainty poses a major concern when planning and operating a hydrocarbon reservoir.

In Jonsbråten (1998) a model for optimizing decisions in oil field operation is developed. The objective is to maximize the expected Net Present Value of the oil field given that the future oil price is uncertain. The problem contains both continuous and binary decision variables, making it a Mixed Integer Programming (MIP) problem. The author uses a stochastic programming approach to the optimization problem, where the uncertain oil price parameter is approximated with a finite scenario aggregation with weighted probabilities. The solution is based on an algorithm called the Progressive Hedging Algorithm, extended to handling MIPs.

Goel and Grossmann (2004) proposes an optimal investment- and operational planning strategy for an offshore gas field. The uncertainty considered in this paper lies in the quality of the reservoirs. Even though seismic data can provide strong indications of the size and deliverability of a reservoir, the measurements are always subject to uncertainty and the truth is not revealed until after big investments have been made. The model proposed by the authors is a multi-stage stochastic program with conditional non-anticipativity constraints, where the objective is to maximize expected NPV. By using a finite scenario approximation for the reservoir uncertainties and a linear reservoir model, it can be solved as a standard Mixed Integer Linear Programming (MILP) problem. Another algorithm based on decomposition is also proposed. Applied to several examples the results are significantly higher expected NPV compared to a deterministic approach, and a lower risk for getting negative NPV values. A similar study were performed by Tarhan et al. (2009) where a duality-based branch-and-bound algorithm was used to solve for the optimal infrastructure of an offshore oil field, with the objective of maximizing expected NPV.

Capolei et al. (2014) introduces a risk oriented approach to production optimization by using the mean-variance (MV) criterion. As distinct from previous work were the expected NPV is maximized in an uncertain environment, the authors here uses a bi-criterion objective function where also the variance (hence the risk) of the NPV is included explicitly. This differs from certainty equivalence optimization and robust production optimization, none of which account for risk directly. The mean-variance optimization strategy is tested in two extensive cases, where the uncertainty lies in the estimated permeability of an oil reservoir. This is realized with 100 potential scenarios, and the optimization problem is solved as an open-loop optimal control problem. The results reveal that the MV approach gives significantly lower risk (i.e. smaller standard deviation in

NPV) with only slightly lower expected return. The authors also propose that the mean-variance rule should be considered in closed-loop reservoir management as well as general Economic Nonlinear Model Predictive Control.

Aanonsen et al. (1995) examines the problem of choosing optimal well locations. This is a very important decision, as the result can have million dollar consequences, but also very difficult due to uncertainties in the reservoir description. The authors begin by presenting some of the core principles in stochastic programming, including expected values and chance constraints. They further present three examples of how to optimize well locations under uncertainty. The first example considers the locations of one injection well and one production well. The uncertainty in the reservoir model is related to the density, length and and sealing effect of small, sub-seismic faults. They are modeled as stochastic variables for transmissibility through the faults, length of the faults and distance between the faults, all of them assumed to have Gaussian probability distributions. The objective is to maximize Expected Net Present Barrels (ENPB). After running 50 Monte Carlo simulations, three equally good maxima are found, all better than the initial guess. Example 2 considers the optimal location of one injection well in a fluvial reservoir where there are already 6 production wells. It is desired that the well hits a channel so that the injection fluid will transport as much oil as possible to the production well, and thus the optimization criterion is expected channel volume between injector and producer. The uncertainty lies in the probability of hitting a channel, and the optimal solution is a trade-off between expected channel volume and the probability of hitting. The example is later expanded to include the chance of blocking faults between the wells. In example 3, the authors look into the uncertainties associated with the deposition of channel sands, with the response variable being ENPB like in example 1.

Deutsch and Srinivasan (1996) address a very interesting technique for handling uncertainties in reservoir models. While it is common to visualize the uncertainty by generating possible *scenarios* or *realizations* of the reservoir, a common problem in practical applications is that only a small number of the available realizations are actually considered. This can be due to the computational effort required to simulate every possible scenario, or the time it takes to professionally inspect all of them, or both. The authors propose a method for *ranking* the available realizations, so that the most important ones (e.g. the expected and bounding cases) can be included in the decision making. To create this ranking, they introduce the concept of a *ranking statistic*, which is a measure to decide whether a realization should receive a high or low ranking. Several ranking statistics are proposed, including simple summary statistics like net-to-gross ratio, net pore volume and average permeability. The idea is that after the realizations have been ranked, only the necessary ones will be used in more extensive simulations. The authors apply this in a synthetic reservoir example with uncertainty in lithology, porosity and permeability. From 250 realizations of the reservoir, five different response variables are proposed as possible ranking statistics, and these are compared to another six statistical ranking measures. They conclude that the net-to-gross ratio is the overall best ranking measure, considering both the true and the statistical ranking. By introducing loss functions they are able to quantify the benefit of using three ranked realizations of the available 250, instead of picking three random ones. The result shows a significant improvement when using the ranked realizations.

Corre et al. (2000) examine the major uncertainties in reservoir management related to geophysics, geology and engineering dynamics. Their approach for handling these is to obtain information about the relevant probability distributions and use it to conduct a risk analysis in order to make better decisions. To provide the basis for the risk analysis, the potential uncertainties are quantified in terms of their impact on a decision criterion through a so-called integrated assessment. This is carried out in a case study, which the authors divide into four major steps. In the first step they obtain the distribution of Gross Rock Volume (GRV). Step two consists of finding the distributions of Original Oil In Place (OOIP) and Original Gas In Place (OGIP). The parameters describing field geometry, seismic facies, rock types and measures of porosity, net-to-gross ratio, permeability and saturation are assumed uncertain. The parameters and their respective uncertainties sets are used as input to a flow simulation software. In step 3 the most relevant realizations from step 2 are extracted using some of the principles covered in Deutsch and Srinivasan (1996), i.e. the 10, 50 and 90 percent quantiles, among others. These are further integrated with uncertainties regarding dynamic parameters in step 4, i.e. permeabilities and faults transmissivity, to name a few. The results that underlie the risk analysis are a probability distribution of final recoverable reserves, statistical cumulative production profiles and probability estimation of product plateau duration.

Da Cruz et al. (2004) introduce the concept of a quality map, which is a 2D representation of the reservoir with regards to several uncertain parameters. The quality map shows how good an area is for production, measured in expected cumulative oil production of a single well after a certain time of production. In an example they show how the quality map incorporates both top depth, oil volume, horizontal permeability and vertical permeability. In a case study the quality map is created from 50 stochastic realizations of a reservoir, and the expected profit is compared to using a single deterministic model. The result is a significant increase when accounting for the uncertainty. However, the result from using a single reservoir representation can be improved by choosing a representative realization from the quality maps. The article also covers ranking of realizations, like Corre et al. (2000) and Deutsch and Srinivasan (1996).

Zafari and Reynolds (2005) use the Ensemble Kalman Filter (EnKF) to assess uncertainties in reservoir description. The EnKF is a subcategory of particle filters that has received increased attention over the last decade, mostly due to its suitable application to large scale problems. Unlike the classic Kalman Filter, the EnKF computes error predictions by using Monte Carlo methods on an *ensemble* of possible state variables. This makes it well suited for handling a large set of reservoir realizations (see Evensen (2003) for a thorough derivation of the EnKF). In a synthetic case study the EnKF is used to estimate several reservoir parameters, with good results. They also show how the EnKF can provide unreliable results when the uncertain parameter has a multimodal probability distribution.

Wang et al. (2009) treat the EnKF as an optimization algorithm rather than a state estimation algorithm. This is compared to more conventional optimization algorithms when solving a closed-loop optimization problem. Here, the steepest ascent algorithm is superior to the EnKF. However, by using the EnKF for data assimilation (like Zafari and Reynolds (2005)) and steepest ascent for the production optimization, the authors are able to estimate reservoir parameters very accurate.

Van Essen et al. (2009) is a highly topical article on Robust Optimization (RO) of oil and gas production under geological uncertainty. They consider an optimal control problem where the objective is to maximize the Net Present Value of a petroleum reservoir by controlling waterflooding, i.e. to delay the water breakthrough and maximize the sweeping. The controlled variables are rates on a number of injection and production wells. The authors explain how the optimal control problem is formulated, and include some theory on the how their optimization algorithm works. A case study is carried out on an oil/water reservoir with eight injection wells and four production wells. The geological uncertainty in the reservoir description is represented by 100 possible scenarios (the realization ensemble), where the fact that no measurements were available makes them equiprobable. Three distinct methods are proposed for the maximization of NPV; a reactive approach, a nominal optimization approach (NO) and a robust optimization approach. In the reactive strategy, the production wells are shut in once the total production is no longer profitable, which is decided to be when the water cut (WC) reaches 87 %. This approach has the advantage of not requiring a system model, but is usually too conservative. The NO approach is deterministic and only considers a single realization, but since no realization is more likely than another the optimization procedure is run on all 100 realizations. The RO approach maximizes the *expected* NPV by considering the entire set of possible scenarios. The solution must be valid for all of the realizations. Based on the results, the probability density functions and cumulative distribution functions for the three solution techniques are approximated. The RO approach has a significantly higher expected NPV than the other two, with a lower variance as well. This is cross-validated on a new and independent set of 100 reservoir realizations, with a very similar outcome confirming the previous finding. The authors emphasize that their conclusions are valid only under the assumption that the realizations ensemble is a good representation of the true reservoir.

Peters et al. (2010) present a summary of a benchmark project conducted for the SPE Applied Technology Workshop on closed-loop reservoir management in June 2008. The purpose of the project was to investigate the combination of flooding optimization and history matching on a synthetic oil field, called the

Brugge field, and propose a closed-loop optimal waterflooding strategy for the future. The geological model of the Brugge reservoir was created in advance by the research organization TNO and contained synthetic well-log data, structure, seismic data and production history for the past 10 years. The task for the participants in the benchmark study (nine different universities/companies) was to estimate certain parameters with history matching, that being permeability, porosity and net-to-gross thickness ratio, in combination with flooding optimization, to provide an optimal waterflooding strategy for the next 20 years. In order to make the strategy closed-loop, the control profiles were tested on the "true" reservoir, evaluated in terms of receiving observations and then updated. Because of practical limitations and time constraints only one iteration was possible, thus the control strategy was divided in two; one for the first 10 years and one for the second (remaining) 10 years. The Brugge field was modeled as a typical North Sea Brent oil field, represented with 20 million grid cells of average size $50 \times 50 \times 0.25$ m. 30 wells were present; 20 producers and 10 injectors. The participants were provided 104 different realizations of the reservoir with respect to facies, porosity, Net-To-Gross ratio (NTG), water saturation and permeability. How the set of realizations was used in the data assimilation, and the method for performing the history matching, varied over the different participants. This was also the case for the optimization part. About one-half of the participants had in common that they performed the optimization in a robust way by considering more than one realization. How these were chosen from the set of history matched scanarios varied from choosing 10 at random, using the mean model to considering the whole ensemble, among others. The results were measured as total realized NPV of the field, and the contributors were also asked to provide the root-mean-squared error of their respective production data. All in all, the results were quite similar, with a spread in order of 10 %. The study clearly showed that those who had used three control intervals per well instead of one gained significantly higher NPV. It also showed that the increase in NPV after the first period observations were given, and the model was updated accordingly, was significant.

Van Essen et al. (2010) extend the Dynamic Real Time Optimization (D-RTO) approach used for production optimization. The authors emphasize that uncertainty in reservoir models typically leads to poor short term predictions, and that this limits the profitability of a general D-RTO approach. They propose a closed-loop combination of D-RTO and MPC, using locally identified, linear models in the MPC. In this way smaller, short term prediction models are combined with the full, long term reservoir model. The MPC controller tracks the reference input, which is desired flow rates on the production wells. The model in the MPC is updated repetitively using a subspace identification method for parameter estimation. A case study is performed on a fictive reservoir model with eight injectors and four producers, where the control target is to maximize NPV. The result from using the proposed control scheme is compared to an open-loop D-RTO approach without MPC tracking, showing a significant improvement (594 M$ against 558 M$) over a time span of 4000 days.

Chapter 5

Case study: Reservoir Optimization

This chapter addresses a case study regarding reservoir optimization. It concerns a fictive oil reservoir, the so-called Egg Model, which has an uncertain permeability field. The objective is to maximize the Net Present Value of the reservoir over a time span of 10 years by using an optimal waterflooding strategy. The control variables are the rate of injected water for the injection wells and bottomhole pressure for the production wells, which is a realistic setting.

The study may be regarded as twofold. In the first part, uncertainty is excluded and the problem is solved as a deterministic optimization problem. This is done in both an output unconstrained and constrained manner. In the constrained example, a base case is included for comparison to reveal the benefit of using mathematical optimization in reservoir management. The second part is about uncertainty handling. The aim is to show the benefit of treating uncertainty explicitly by optimizing over multiple realizations. All simulations are done in MATLAB 2014a with MRST 2014a and problem setups from the REMSO optimization toolbox. The optimization is performed with Single Shooting using the IPOPT software[1]. The computer used for conducting the simulations is a HP Optiplex 9020 desktop with an Intel Core i7-4770 @ 3.4 GHz processor and 16 GB RAM.

5.1 The Egg Model

The Egg Model is a synthetic reservoir model developed by Maarten Zandvliet and Gijs van Essen as a part of their PhD theses at the Delft University of Technology (Jansen et al., 2014). It has been used in several research publications on reservoir management and oil and gas production optimization. The Egg Model consists of a 60 × 60 × 7 grid structure, where the active cells form an egg-like shape. It is a channelized oil-water reservoir with 12 wells total; eight injectors and four producers. To represent the uncertainty related to the permeability, the Egg Model includes 100 additional realizations of the permeability field, making the model well suited for work on uncertainty handling. The Egg Model is available for download at the 3TU.Datacentrum repository, [2] and includes files for supporting all of the most widely recognized reservoir simulators. Table 5.1 summarizes some of the important reservoir properties. An extended list can be found in Jansen et al. (2014). Notice that the injectors are controlled by rate and the producers by BHP.

The Egg Model is simplified in this work to reduce the computational effort required for simulation. This is done by removing six of the seven horizontal layers that comprise the reservoir, reducing the model total size with a factor of seven. Figure 5.1 displays the single layer Egg Model along with the different well positions. Notice the highly permeable channels going in the vertical direction.

[1] https://projects.coin-or.org/Ipopt

[2] http://data.3tu.nl/repository/uuid:916c86cd-3558-4672-829a-105c62985ab2

Table 5.1: Reservoir properties for the Egg Model

Property	Value	SI unit
Grid block height	4	m
Grid block length	8	m
Grid block width	8	m
Porosity	0.2	-
Initial reservoir pressure	$40 \cdot 10^6$	Pa
Initial water saturation	0.1	-
Water injection rates	79.5	m^3/day
Production well bottom hole pressures	$39.5 \cdot 10^6$	Pa

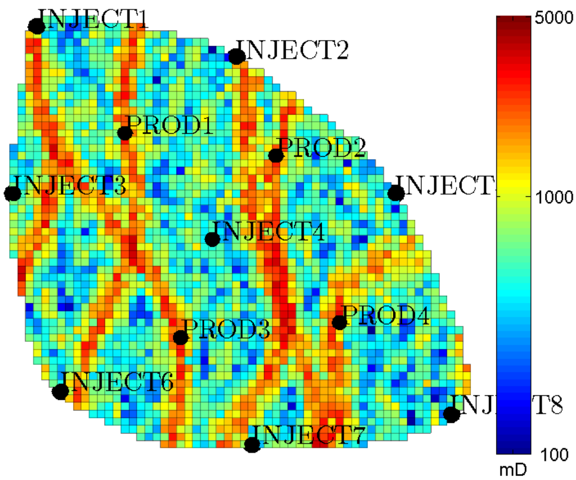

Figure 5.1: Permeability plot of the simplified Egg Model

5.2 Case 1: A deterministic optimization approach

The deterministic case study is done by selecting only one permeability realization. There is no information available that can be used to rank the realizations, thus they are considered equiprobable. In this section, realization number 50 is chosen from the ensemble of 100. The purpose of the deterministic case study is to show the application of MRST and REMSO/IPOPT to find an optimal waterflooding strategy for a realistic reservoir model, and evaluate the solution over the 10 year production period.

5.2.1 Output unconstrained problem

Consider first an output unconstrained formulation, meaning the well output variables are unbounded. The control input is constrained, as this has little effect on the simulation time. The prediction horizon is partitioned in $K = 150$ steps of unequal length, the first steps being 1, 4, 10 and 15 days and the remaining steps all being 30 days. One year is considered to be 360 days in this case study. The control horizon is divided into $U = 10$ equal periods of 360 days, meaning the wells are adjusted once a year. As there are 12 wells, the control vector has dimension $u \in \mathbb{R}^{12}$, where the first eight entries are the water injection rates and the remaining four are the producer bottom hole pressures. The state vector contains the reservoir pressure and water saturation for all grid cells (i.e. two states per grid cell). The single layer Egg Model contains 2491 active grid cells, thus the state vector has the dimension $x \in \mathbb{R}^{4982}$. The vector of algebraic variables contains output water rate, oil rate and bottomhole pressure for all 12 wells, i.e. $v \in \mathbb{R}^{36}$. For the initial conditions on the state and control vector, the values from Table 5.1 are used, i.e. $x_0 = [400,\dots,400,0.1,\dots,0.1]^\top$ and $u_0 = [79.5,\dots,79.5,395,\dots,395]^\top$ where the pressures are scaled to bars. The lower bounds on the control vector are 2 Sm^3/day for the injectors and 380 bars for the producers, whereas the corresponding upper bounds are 500 Sm^3/day and 420 bars, i.e. $b_l^u = [2,\dots,2,380,\dots,380]^\top$ and $b_u^u = [500,\dots,500,420,\dots,420]^\top$. The pressure state is bounded below with zero, but has no upper bound. The saturation is constrained to be in the interval $[0,1]$. Thus, $b_l^x = [0,\dots,0,0,\dots,0]^\top$ and $b_u^x = [\infty,\dots,\infty,1,\dots,1]^\top$. As this section considers an output unconstrained formulation, there are no bounds on v. Using the framework from Section 3.2.3, the optimization problem is formulated as

$$\min_{u \in \mathbb{R}^{12}} \quad \sum_{k \in \mathcal{K}} J_k(v_k, u_{\kappa(k)}) \tag{5.1a}$$

$$\text{subject to} \quad x_{k+1} = R^x(x_k, u_{\kappa(k)}), k \in \mathcal{K} \tag{5.1b}$$

$$v_k = R^v(x_k, u_{\kappa(k)}), k \in \mathcal{K} \tag{5.1c}$$

$$b_l^x \leq x_k \leq b_u^x, k \in \mathcal{K} \tag{5.1d}$$

$$b_l^u \leq u_{\kappa(k)} \leq b_u^u, k \in \mathcal{K} \tag{5.1e}$$

where $J(v, u)$ is the negated NPV, calculated from Eq. (3.2) with $r_o = 1.0$, $r_w = 0.01$, $r_i = 0.01$ and $b = 0$. That is, no discount factor is included in this study. The NPV values are later scaled to represent an oil price of 65 USD/STB which is the Brent Crude price at the time of writing.

Solution

The solution algorithm is set up to terminate when reaching a convergence tolerance of 10^{-7} or 100 iterations. In this case the maximum number of iterations is reached, meaning the algorithm has not converged to a local optimum under the given tolerance. However, a feasible solution is found. To evaluate this solution, the reservoir is simulated again for this control input. The result is displayed in Figure 5.2, showing the well outputs from the first producer (the rates are converted to STB/day). The graphs reveal some strange behavior, with negative production rates of both oil and water. A negative oil production means that the producer is "creating" oil and injecting it into the reservoir. The reason this happens is that when there are no output constraints, the algorithm finds it lucrative to inject created oil and produce it at a later time. When a well is producing mostly water, it is also beneficial for the solver to invert the output to turn the costs of producing water into profits. This is obviously not possible in reality, thus the unconstrained solution is not implementable, nor does it provide us with useful insight. Output plots for the remaining wells are enclosed in Appendix B.1.

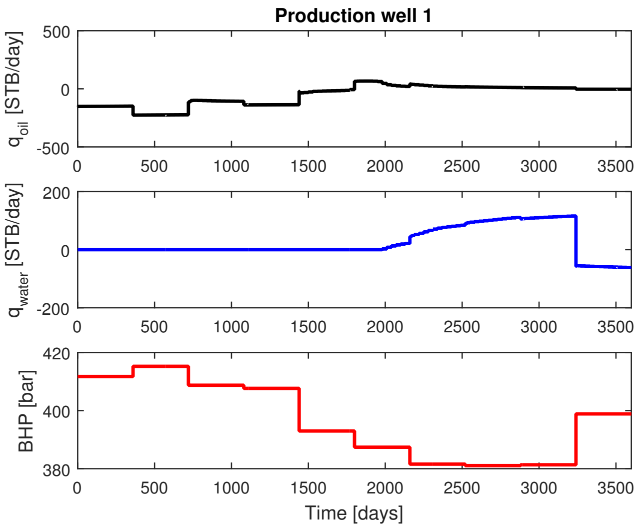

Figure 5.2: Unconstrained output plot from Producer 1

5.2.2 Output constrained problem

In this section, constraints on the well outputs are added to the optimization problem (5.1). This involves a minimum oil production rate of 2 Sm^3/day ($\approx$ 12.6 STB/day) and a minimum water production rate of 0 Sm^3/day. The injection wells are not given any output constraints (i.e. no bounds on the bottom-hole pressure). The output constraints are implemented as bounds on v, i.e.

$b_l^v = [-\infty,\ldots,-\infty,0,\ldots,0,-\infty,\ldots,-\infty,2,\ldots,2,-\infty,\ldots,-\infty,-\infty,\ldots,-\infty]^\top$ and

$b_u^v = [\infty,\ldots,\infty,\infty,\ldots,\infty,\infty,\ldots,\infty,\infty,\ldots,\infty,\infty,\ldots,\infty,\infty,\ldots,\infty]^\top$. Since v contains the water injection rates and the producer BHP's, which are both controlled variables with constraints in u, these are not constrained in v to prevent unnecessary adjoint computations (by setting them to $\pm\infty$ the algorithm removes them). The problem is solved using the same formulation as in Section 5.2.1 with the additional constraints on ν, and the same algorithm options. Also here the maximum number of 100 iterations is reached instead of the given tolerance of 10^{-7}. As the algorithm has not converged to a local optimum, the solution is by definition not optimal. It will, however, be referred to as "the optimized" solution here. To evaluate the optimized solution, a base case is also included for comparison. The base case is created by setting a constant water rate of 2 Sm^3/day on the injectors and a constant bottomhole pressure of 400 bars on the producers. The resulting outputs from Producer 1 are depicted in Figure 5.3, a full overview of the simulation results is found in Appendix B.2.

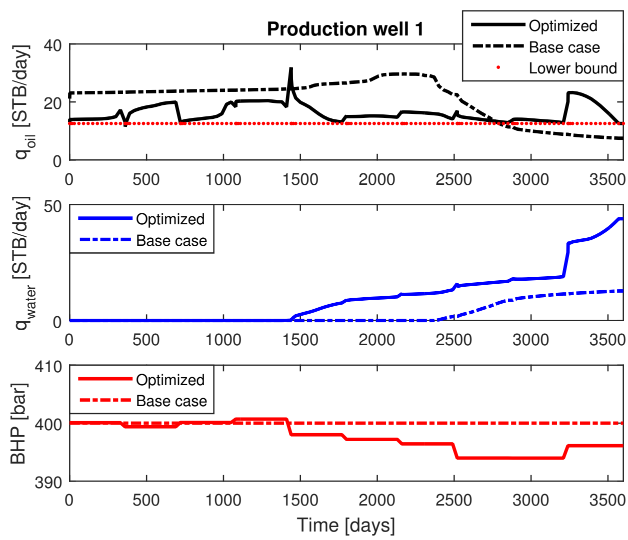

Figure 5.3: Constrained output plot from Producer 1

As seen, the negative output rates are gone, and the plots provide a realistic production scenario. Looking at the top graph, the oil production in the base case lies higher than the optimized case for more than seven years. The base case also produces less water. For the optimized solution, the bottomhole pressure drops as the total production increases from around 1500 days, which is consistent. During the last year, the oil production drops significantly while the water production increases, indicating a water breakthrough at around 3240 days. The base case solution does not account for output constraints, and is seen to violate the lower bound of 2 Sm^3/day (12.6 STB/day) at around 2800 days. However, it does not go below zero, so the violation does not cause an issue. Figure 5.4 shows the total production of oil and water (i.e. summed over all four producers), revealing that the optimized solution produces significantly more of both. Furthermore, Figure 5.5 shows the development in NPV for the two cases, where the y-axis values have been scaled according to an oil price of 65 USD/STB. A clear increase in NPV is seen all the way through the time horizon, with a flat out at the very end, which is recognized as a positive curvature. Again, the optimized solution has a clearly better return, showing the potential gain in using mathematical optimization in oil and gas production. Finally, Figure 5.6 plots the water saturation at six different times during the 10 year production period. Notice how the waterfronts spread out from the injectors towards the producers.

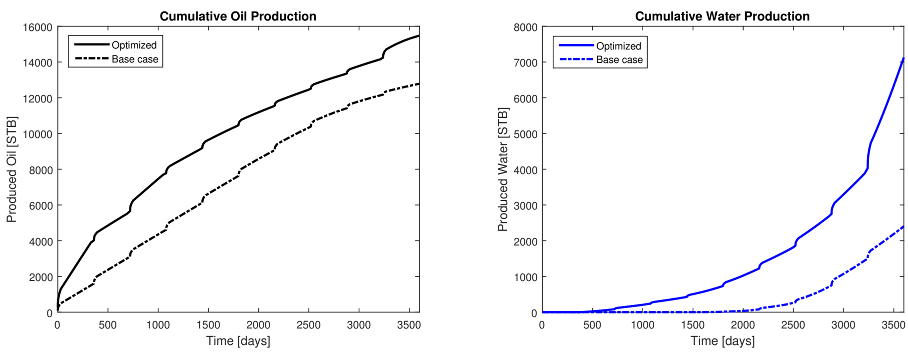

Figure 5.4: Total production plots for the constrained case

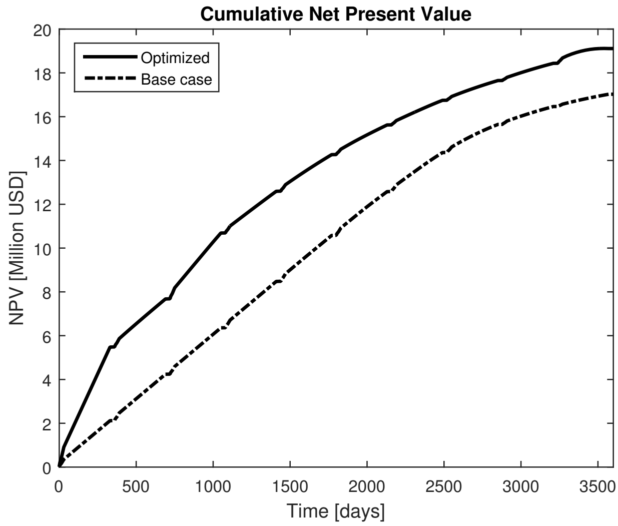

Figure 5.5: Net Present Value for the constrained case

5.3 Case 2: Optimization with multiple realizations

As described in Section 5.1, the permeability of the Egg Model is uncertain, which is represented with an ensemble of 100 realizations. In this section, the theory presented in Sections 3.3-3.4 is applied to the Egg Model, with intent to show the benefit of using stochastic programming in a realistic reservoir optimization scenario. Because of the extreme computational effort required for doing a full optimization on all 100 realizations, only the 10 first are used in this study. This is considered enough to demonstrate the principles, and can easily be extended to include the whole ensemble. The solutions are still evaluated for all 100 realizations, as this only requires simulation and not optimization. Moreover, as the output unconstrained case in Section 5.2 provided a practically infeasible solution, a purely unconstrained case is not included in the multiple realizations examples.

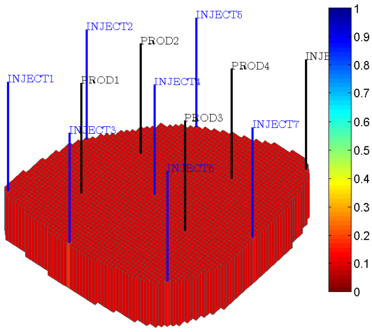

(a) 1 day

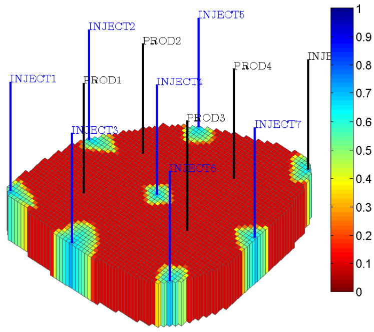

(b) 1 year

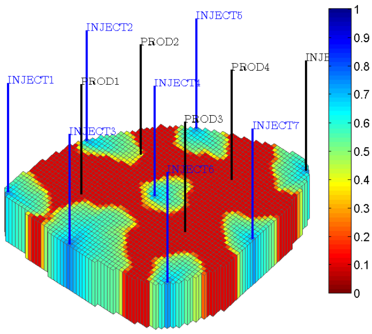

(c) 3 years

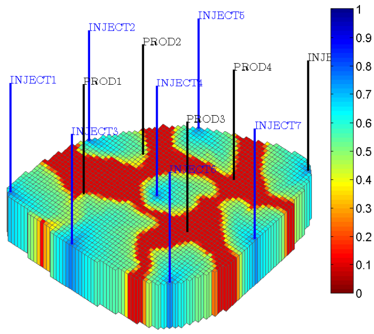

(d) 5 years

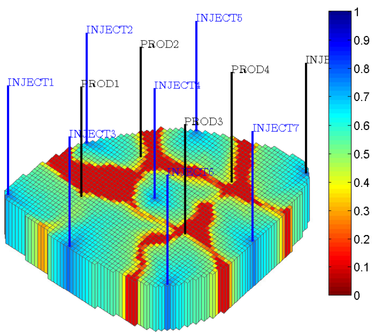

(e) 7 years

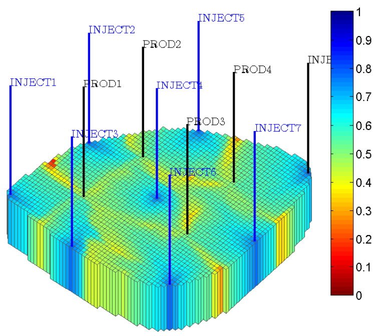

(f) 10 years

Figure 5.6: Water saturation as the Egg field is produced

5.3.1 Evaluating the deterministic solution

The deterministic solution from Section 5.2.2 is found by considering only one realization of the permeability. Let us now see how this solution performs when simulated for all 100 realizations, that is, how it performs when evaluated on an uncertain reservoir model. Figures 5.7-5.8 contain the 100 different outcomes of Producer 1 and Injector 1, where the black lines are the mean values of the respective variables. Observe that roughly 50 % of the predicted oil production scenarios are infeasible with negative rates. As this cannot happen in reality, it proves the fact that the deterministic solution will have a very unpredictable outcome. The output bottomhole pressure on Injector 1 is reasonable for all scenarios. The output plots from the other wells are enclosed in Appendix B.3.

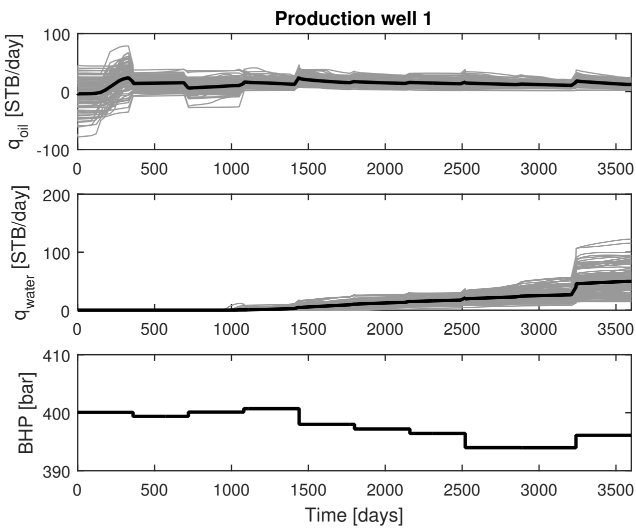

Figure 5.7: Producer 1 for the deterministic solution

Figure 5.9a plots the development in NPV over the time horizon, scaled with a factor corresponding to an oil price of 65 USD/STB. There is an evident spread among the scenarios, and after 10 years the difference between the highest and lowest cumulative NPV is more than three million USD. Over a time span of 10

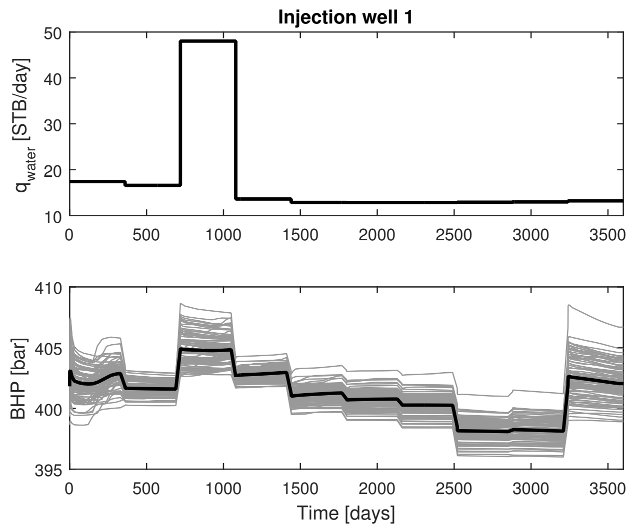

Figure 5.8: Injector 1 for the deterministic solution

years it is, however, hard to say if this is significant or not. Figure 5.9b shows a histogram plot of the final NPV (after 10 years). The distribution is reminiscent of a normal distribution. The expected NPV after 10 years is 17.51 million USD, and the standard deviation is 0.68 million USD.

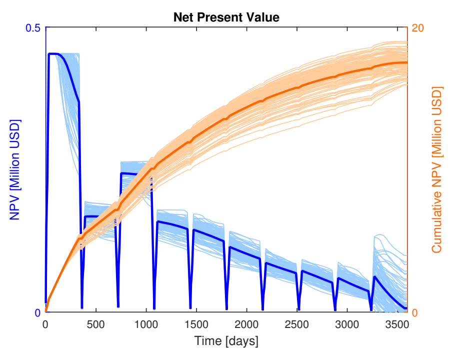

(a) NPV development

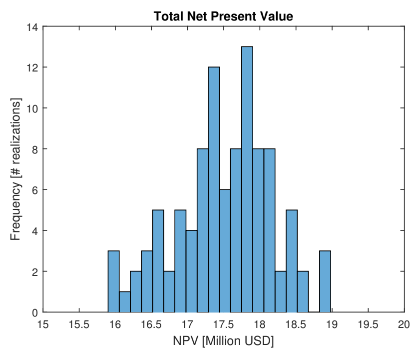

(b) NPV after 10 years

Figure 5.9: Net Present Value for the deterministic solution

5.3.2 Robust solution

The deterministic optimization problem has the objective of maximizing the Net Present Value of the Egg field over the 10 year prediction horizon. However, the control profile that maximizes the NPV of one reservoir realization will probably not maximize the NPV of the next realization. Thus, as explained in Ch. 3, what we seek is the control profile that maximizes the expected NPV over the whole ensemble. Since the realizations of the Egg Model are considered equiprobable, the Sample Average Approximation applies in this case. Moreover, as discussed in Section 3.5, there are several ways to handle output constraints when optimizing on multiple reservoir realizations. Because an unconstrained formulation resulted in negative output flow rates, which cannot happen in reality, this section considers the *robust* or *worst case* formulation, where one requires that the constraints are satisfied for all realizations. In this case it means that there can be no negative rates for any of the scenarios. The robust optimization problem is formulated using the framework from Section 3.5.1, with $N_r = 100$. The prediction and control horizons are the same as in problem (5.1), as well as the bounds on the control input and state vector.

$$\min_{u \in \mathbb{R}^{12}} \quad \frac{1}{100} \sum_{n=1}^{100} \sum_{k \in \mathcal{K}} J_k(v_{k,n}, u_{\kappa(k)}) \tag{5.2a}$$

$$\text{subject to} \quad x_{k+1,n} = R_n^x(x_{k,n}, u_{\kappa(k)}), \; k \in \mathcal{K}, \; n = 1, ..., 100 \tag{5.2b}$$

$$v_{k,n} = R_n^v(x_{k,n}, u_{\kappa(k)}), \; k \in \mathcal{K}, \; n = 1, ..., 100 \tag{5.2c}$$

$$b_l^x \le x_{k,n} \le b_u^x, \; k \in \mathcal{K}, \; n = 1, ..., 100 \tag{5.2d}$$

$$b_l^v \le v_{k,n} \le b_u^v, \; k \in \mathcal{K}, \; n = 1, ..., 100 \tag{5.2e}$$

$$b_l^u \le u_{\kappa(k)} \le b_u^u, \; k \in \mathcal{K} \tag{5.2f}$$

The actual implementation has $N_r = 10$, i.e. only the first 10 realizations are used for the optimization. The algorithm is set up with a convergence tolerance of 10^{-7} or 100 iterations. Again, the maximum number of iterations is reached before the convergence condition. The solution is then simulated for all 100 realizations as in Section 5.3.1. The predicted production scenarios are shown in Figure 5.10. The produced oil graph has a clearly lower spread than for the deterministic solution in Figure 5.7. Even though the solution is based on only 10 realizations, there are almost no negative output rates. It is interesting, however, that the robust solution actually gets a few scenarios with negative water production, whereas the deterministic solution has none. There is, on the other hand, no guarantee that this would be the case if the deterministic solution was based on any other realization in the ensemble. The injection plot in Figure 5.11 looks somewhat similar to Figure 5.8. The bottomhole pressure is slightly higher in the robust case. The remaining well plots are enclosed in Appendix B.4.

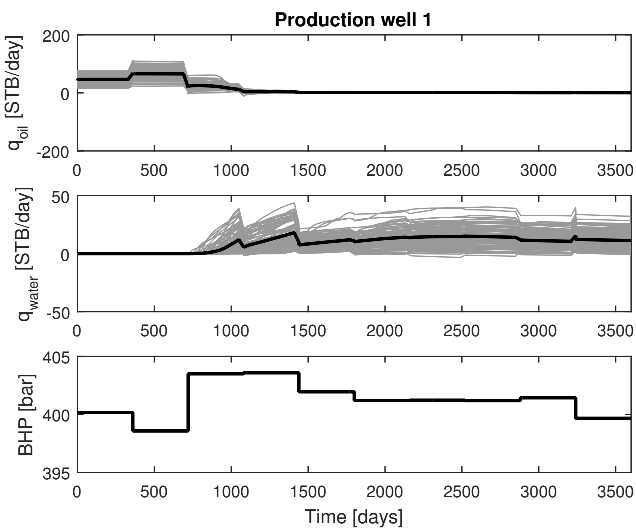

Figure 5.10: Producer 1 for the robust solution

The NPV development and final NPV histogram are displayed in Figure 5.12. The cumulative NPV graph is seen to have lower spread than for the determin-

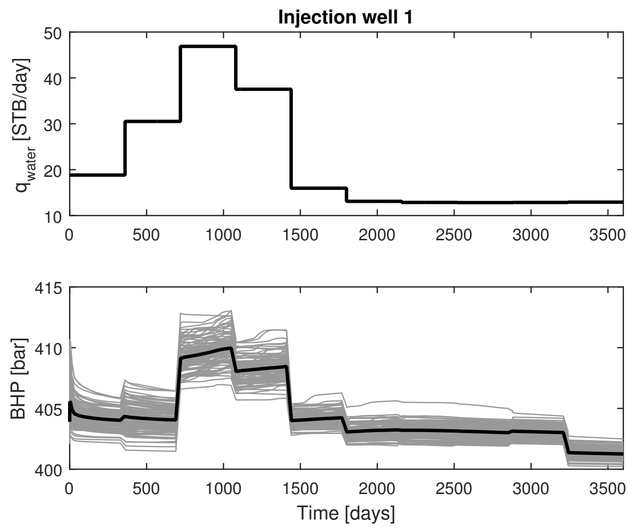

Figure 5.11: Injector 1 for the robust solution

istic solution, and the development is the same for all scenarios for about 1000 days. The difference between the highest and lowest final NPV scenario is 1.64 million USD. From Figure 5.12b, the distribution looks like a skew normal distribution. The expected NPV at the end of the 10 year production period is 19.15 million USD with a standard deviation of 0.44 million USD.

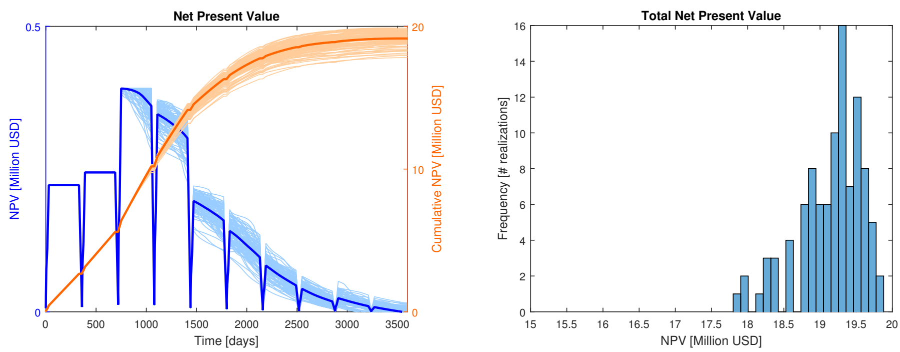

(a) NPV development

(b) NPV after 10 years

Figure 5.12: Net Present Value for the robust solution

5.3.3 Comparison of solutions

Figure 5.13 shows the average total amounts of produced oil, produced water and injected water for the 10 year period. The robust solution is seen to yield a slightly higher total production on average of both oil and water, but also requires 2000 barrels more of injected water. However, this bar plot does not show the spread in the respective values, thus it does not provide very much insight. In addition, the negative oil production from the deterministic solution will have a negative contribution to the total production figure.

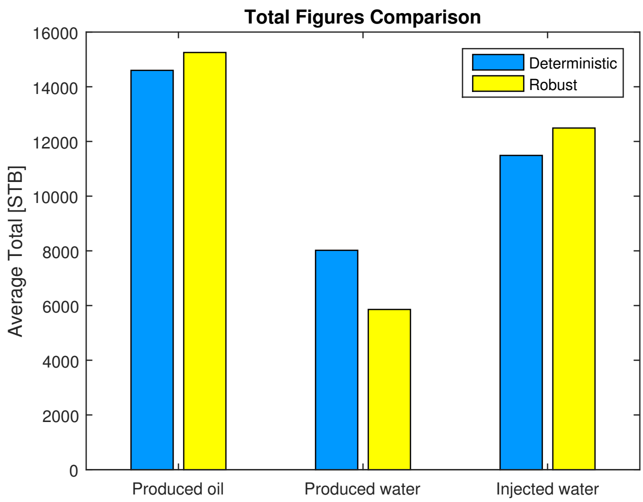

Figure 5.13: Average total production/injection figures for the deterministic and robust solutions

The optimization target in this case study is the Net Present Value of the Egg reservoir. Thereby, the NPV plots for the two approaches are directly comparable, and give reliable pictures of how well they perform. Figure 5.14 shows the cumulative NPV graphs for the deterministic and robust solution plotted together. The upper and lower dotted lines are the 90th and 10th quantiles, respectively. The robust solution has a more desirable curvature, as the steeper increase means the production is generating profits faster. The curve is almost flat at the end of the prediction horizon, meaning the field's profitability has reached a maximum (with the given configuration).

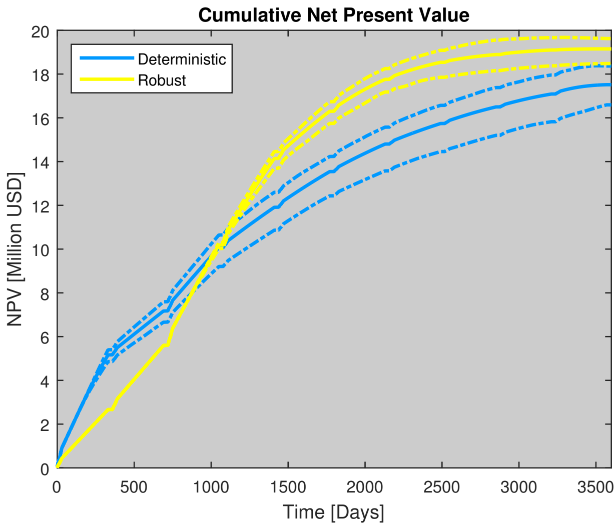

Figure 5.14: Cumulative NPV plots for the deterministic and robust solution. The dotted lines are the 90th and 10th quantiles of the respective distributions

Furthermore, Figure 5.15 shows the histograms for the final NPV values together. The robust solution has a clearly higher expected NPV (1.63 million USD) than the deterministic, as well as lower variance. A box plot can provide a deep comparison, and has sometimes better readability than the histogram. Looking at Figure 5.16, the red lines are the medians of the final NPV for the robust and deterministic solution. The blue boxes around the medians are defined by the 25th and 50th quantiles, i.e., 50 % of the probability masses are contained in the boxes. The dotted lines lead to the respective maxima and minima. Notice how the quantiles are tighter wrapped around the median for the robust solution. Also, the box plot clearly shows that the median for the robust solution is better than the best case scenario for the deterministic solution. All in all the robust solution appears superior to the deterministic.

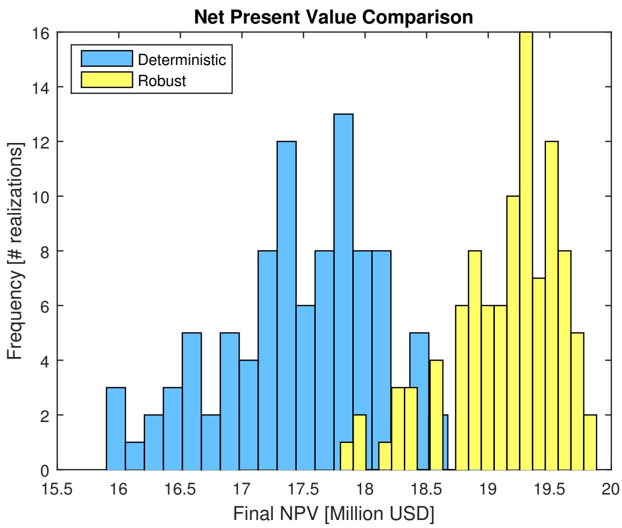

Figure 5.15: Histogram plots of the NPV at the end of the production period

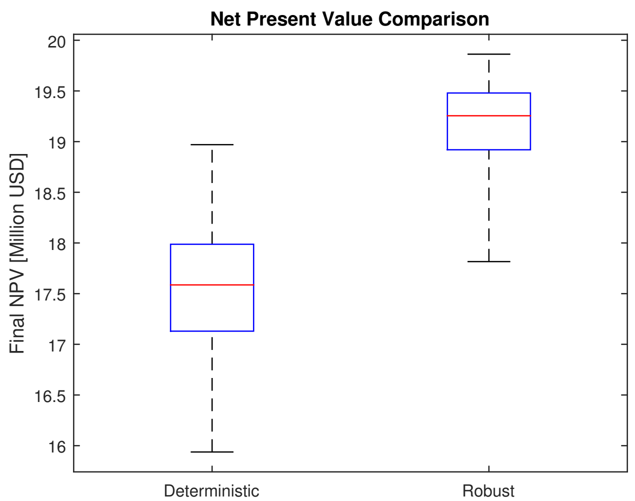

Figure 5.16: Box plot comparison of final NPV for the two solutions

Comparing constraint violations

The preceding comparison shows that optimizing over the realizations ensemble gives a solid increase in expected Net Present Value. Furthermore, Figure 5.17 shows an overview of how many production scenarios that contain one or more instances of negative rates, for the deterministic and robust solution. Even though the robust solution is based on only 10 realizations, there are very few constraint violations for the oil production, cf. Figure 5.17a. For Producer 1, the robust solution has 8 scenarios that breach the zero border, whereas the deterministic solution has 55. For Producer 2, the robust solution has 8 violations and the deterministic has none. For Producer 3 and 4, the robust solution has only valid scenarios, whereas the deterministic solution has 49 and 29 violations, respectively. For the water production, however, the deterministic solution gives only one scenario on Producer 4 with negative rates, cf. Figure 5.17b. The robust solution has 8 and 13 for Producer 1 and 2, respectively, and none for Producer 3 and 4. Note that the y-axes are scaled differently in the oil and water case. It is also important to remember that the outcomes could be very different if the deterministic solution was based on any other realization.

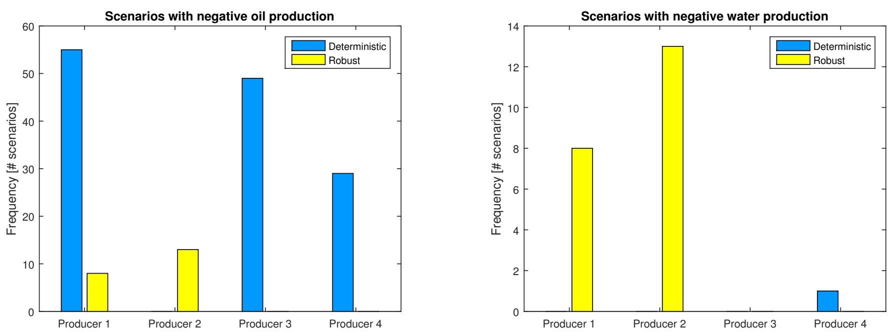

(a) Oil (b) Water

Figure 5.17: Bar plot comparison of scenarios with negative production

The most important results from this section are gathered in Table 5.2.

Table 5.2: Results of the stochastic case study

			Deterministic	Robust
Expected NPV (million USD)			17.51	19.15 (+ 11.4 %)
Standard dev. NPV (million USD)			0.68	0.44 (- 35.3 %)
Constraint violations (# scenarios)	Oil	Prod. 1	55	8
		Prod. 2	0	13
		Prod. 3	49	0
		Prod. 4	29	0
	Water	Prod. 1	0	8
		Prod. 2	0	13
		Prod. 3	0	0
		Prod. 4	1	0

Chapter 6

Discussion

6.1 Result evaluation

6.1.1 Deterministic case, output unconstrained

The case study in Ch. 5 considers first a deterministic problem formulation, i.e. a formulation considering a single realization of the reservoir, with no output constraints. The solution algorithm does not converge within the given limit of 100 iterations. By inspection of the progress log provided by the algorithm, the tolerance of 10^{-7} is too tight for the solution to converge in 100 iterations. A tolerance set to 10^{-4}, on the other hand, would have given convergence. For an economic objective function like Net Present Value, which has unit USD, 10^{-4} is considered tight enough to call the solution a local optimum. Hence, 10^{-4} would be a better choice of convergence tolerance in this case. However, a feasible solution is still found from the 100 iterations. This solution, here referred to as the "optimized" solution, results in a production scenario with negative rates on oil and water. This happens because the unconstrained formulation enables the solver to "create" oil that can be produced again at a later time. Recalling Figure 5.2, the water production becomes negative at the last control period (i.e. 3240 days). Because the NPV formula (3.2) penalizes water production, the solver inverts the well output towards the end when the water cut is high, thereby turning the costs into profits. As one of the main purposes of doing reservoir simulation is to gain insight to the problem and learn about the reservoir, the unconstrained solution is rather useless.

6.1.2 Deterministic case, output constrained

In the unconstrained case in Section 5.2.1, the problem is that the solution yields negative output rates, which will never happen in reality. Thus, in order to provide realistic production scenarios, the output rates must be constrained to positive values. Theoretically, a negative production means that the bottomhole pressure in the producer is lower than the reservoir pressure, which is technically possible, but unlikely and most importantly unwanted. The fact that the solver "creates" oil and water is impossible, of course, so the negative rates must be prohibited. Thus, the deterministic problem is extended with lower bounds on the oil and water production. The solution algorithm is set up with the same tolerance of 10^{-7}, which again is too tight for the solver to converge. The optimized solution is simulated together with a base case using a constant BHP on the producers and a constant water rate on the injectors. Recalling Figure 5.7, the oil production for both solutions is less than 40 barrels a day for the whole prediction period. This is considered low. For comparison, several oil fields in the North Sea have wells that deliver more than 10 000 barrels a day. This is somewhat irrelevant as the Egg Model is a fictive reservoir and the production figures cannot be directly compared to real-life fields. Moreover, the Egg model is simplified in this case study, resulting in even lower outputs than if all seven layers are included. Furthermore, the results reveal that the optimized solution gives increased return compared to the base case, here in terms of an increased final NPV of 2 million USD, or approximately 12 %. In terms of the real oil industry, this is a huge improvement implying a multi-million (or even multi-billion) dollar benefit. If all seven layers of the Egg were included, there is reason to believe the enhancement would have been even greater. However, also here it is important to keep in mind that the Egg Model is a fictive reservoir, and the results here might not be obtainable in a real oil field application. Nonetheless, the numbers do demonstrate the possible gain in using mathematical optimization in reservoir management.

6.1.3 Stochastic case

In Section 5.3 the uncertainty in the Egg Model's permeability field is included in the analysis. When evaluating the deterministic solution, which is based on only one realization of the permeability, over the whole ensemble of 100 realizations, it turns out that more than 50 % of the scenarios have negative oil production. That is, the uncertainty renders the deterministic solution unimplementable with more than 50 % probability. This is, of course, under the assumption that one of the realizations in the ensemble is the "real" reservoir and that they are all equiprobable (see Section 6.2). What would actually happen if the deterministic solution was attempted implemented is hard to say, it might just have been impossible to achieve the requested bottomhole pressures, or they might cause other outputs than predicted. Regardless, the results in this report show that uncertainty can have big impacts on the production performance, and that it causes major feasibility issues. To prevent the negative production under the uncertain conditions, the robust formulation requires the outputs to be positive for all realizations considered. This would normally be the whole ensemble, but is restricted to 10 realizations in this work to reduce the computational effort required for including them all. It also maximizes the expected NPV over the ensemble subset. The robust solution is also simulated for all 100 realizations, and the results are remarkable. Recalling Figure 5.14, the robust solution yields an increase in expected final NPV of another 1.64 million USD, or 11.4 %, which is nothing else but exceptional. Again, given that the Egg Model is not a real reservoir, this might not be obtainable in an actual application. In addition, as clearly seen from Figure 5.15, the variability in the final NPV is significantly lower for the robust solution. It is often desirable to reduce the spread in possible outcomes when dealing with uncertainty, thus the lower variance is considered a strength. In applications that are especially sensitive to variations, the variance may be included in the objective function as a trade-off with the expected value. This is called the mean-variance functional (see Capolei et al. (2014) or Ch. 4). In this case, the variance is not explicitly included, but is still reduced as a result for incorporating the uncertainty. Furthermore, by comparing constraint violations, the robust solution is seen to give very few scenarios with negative production, cf. Figure 5.17. If all 100 realizations had been used in the optimization, the robust solution would have had none, obviously. In this way, the robust problem formulation has removed the feasibility issues with the deterministic solution, in addition to giving increased expected return with higher confidence. Since the optimization problem as formulated in Ch. 5 makes it optimal with negative production if unconstrained, the robust or worst case decision criterion is the only one that is reasonable to use. It makes no sense to allow negative rates in a certain percentage of the scenarios, thus the CVaR formulation is inappropriate for this type of constraint. CVaR is better suited for handling upper bounds, see Section 7.2.

6.2 Assumptions

Some important assumptions are made for the case study in Ch. 5. First off, the uncertainty is related to the permeability only. In real reservoir management applications, there are uncertainties attached to several other rock (and also fluid) parameters. Hanssen et al. (2014) consider uncertainties in the Gas Oil Ratio (GOR) and water cut of wells, for instance (see Ch. 4 for a summary). The future oil price is another example of a parameter that is highly uncertain in reality. Jonsbråten (1998) includes this in the analysis (see Ch. 4). Incorporating uncertainties from multiple sources complicates the optimization problem, and so it is not uncommon to consider only the main sources of uncertainty that have the most impact on the objective. Given that the uncertain parameter is the permeability, this work uses a given set of 100 realizations that is downloaded together with the rest of the model. That is, no consideration is given to how the realizations are created, and they are therefore assumed to be equiprobable. As mentioned in Section 6.1, the result interpretations are based on the assumption that one of the realizations in the ensemble is the real permeability field. In a real application, this will almost certainly never be true, and we can never know what the actual reservoir looks like exactly. The point of the realizations ensemble, however, is for it to be comprehensive enough to be a good representation of the uncertainty, even though a discretization can never reproduce an exact picture of reality, only an approximation.

Chapter 7

Conclusion

7.1 Summary and concluding remarks

This thesis addresses reservoir management, with particular focus on how to account for uncertainty when performing control optimization. An introduction to reservoir simulation is given, covering the most central building blocks of a geological model and the fundamental differential equations for describing multi-phase fluid flow in porous rocks. The reservoir management concept is explained, and the strong relation to production optimization is clarified. The reservoir control optimization problem is defined, with a brief overview of solution methods. Stochastic programming theory is introduced, emphasizing the main difference from deterministic optimization. A literature review on previous work done on reservoir management under uncertainty is performed. The covered theory is applied in a case study on reservoir optimization. The reservoir encountered is the famous Egg Model, simplified to reduce computational load. The reservoir model has uncertainty attached to the permeability, represented with an ensemble of 100 realizations. The problem is first solved as a deterministic optimization problem considering a single realization. The solution is then evaluated over the full set of realizations, which yields unrealistic production scenarios with many constraint violations. A new solution based on multiple realizations is found, using a robust treatment of output constraints. By comparison, the robust solution is seen to give higher expected return, lower variability and almost no constraint violations.

Based on the covered theory and the results obtained in this thesis, it is concluded that stochastic programming is superior to its deterministic counterpart in reservoir optimization problems containing uncertain parameters. The framework enables a highly structured approach to complex problems, where the decision maker can choose what the desired statistical property of the solution is. By optimizing over the realizations ensemble, the robust solution is able to increase the expected final Net Present Value with 11.4 %, which in a real oil field application could imply several billion dollars over 10 years. Stochastic programming also offers a very elegant way of handling output constraints when they are affected by uncertainty. With the chance constraint approach, the degree of risk aversion can be directly controlled with the α parameter. This is a very powerful tool not only in production optimization, but also in all kinds of business planning. With the tight oil market as seen at the time of writing, risk management is crucial, and stochastic programming is highly applicable to this discipline.

7.2 Recommendations for further work

Stochastic programming allows for explicit treatment of uncertainty in optimization problems. In the case study in Ch. 5, this is used to require the output rates to be non-negative for all realizations included. But, as explained in Ch. 3, stochastic programming can also be used to control risk. This can be implemented, for example, through the CVaR measure. However, because it never makes sense to allow negative production rates, the CVaR approach is not suited for the problem encountered here. When solving the robust optimization problem, no upper bounds are set for the producer outputs. Even though the obtained production rates are well within reasonable limits, it would be a natural extension of the problem to include an upper processing capacity constraint for the total water production. For this type of constraint, the CVaR or any other probabilistic criterion would be a very suitable candidate for the violation handling. Future work on stochastic reservoir control optimization should consider a problem formulation where the lower bounds are treated in a robust fashion, and the upper bounds are treated in a probabilistic manner where the conservativeness can be directly controlled.

Appendix A

Acronyms

CDF Cumulative Distribution Function

CLRM Closed-Loop Reservoir Management

CVaR Conditional Value-at-Risk

D-RTO Dynamic Real-Time Optimization

E&P Exploration & Production

EnKF Ensemble Kalman Filter

EOR Enhanced Oil Recovery

GOR Gas Oil Ratio

GRV Gross Rock Volume

IID Independent Identically Distributed

IVP Initial Value Problem

MILP Mixed Integer Linear Programming

MIP Mixed Integer Programming

MPC Model Predictive Control

MRST Matlab Reservoir Simulation Toolbox

MS Multiple Shooting

MV Mean-Variance

NLP Nonlinear Programming

NO Nominal Optimization

NPV Net Present Value

NTG Net-To-Gross

OGIP Original Gas In Place

OOIP Original Oil In Place

PDF Probability Density Function

PEBI Perpendicular Bisector

PID Probportional-Integral-Derivative

RO Robust Optimization

SAA Sample Average Approximation

SS Single Shooting

STB Stock Tank Barrel

VaR Value-at-Risk

WC Water Cut

Appendix B

Simulation results

B.1 Extended results from Section 5.2.1

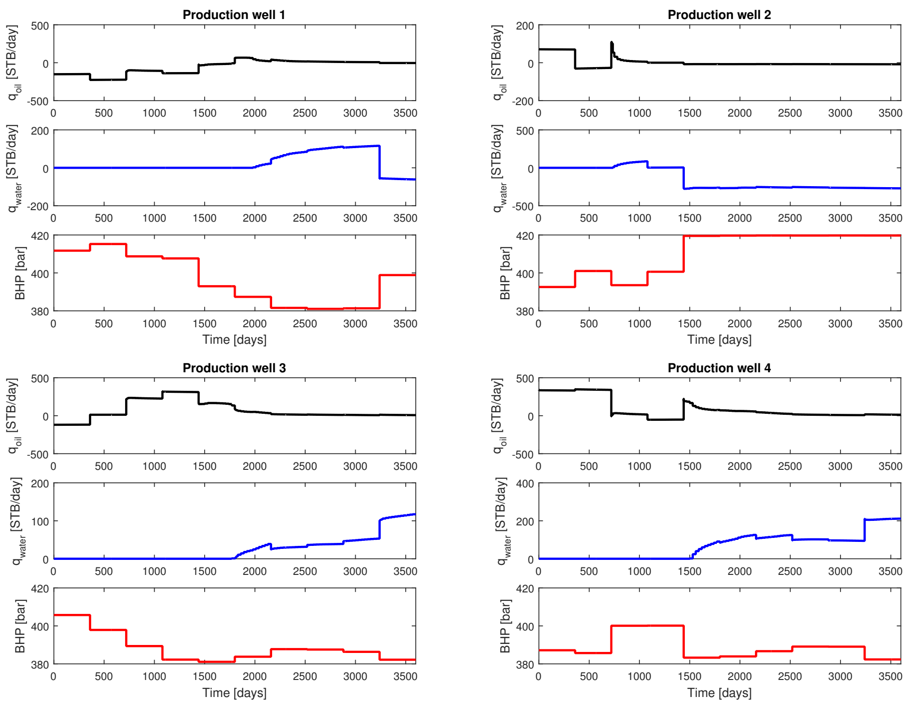

Figure B.1: Unconstrained output plot from the four producers

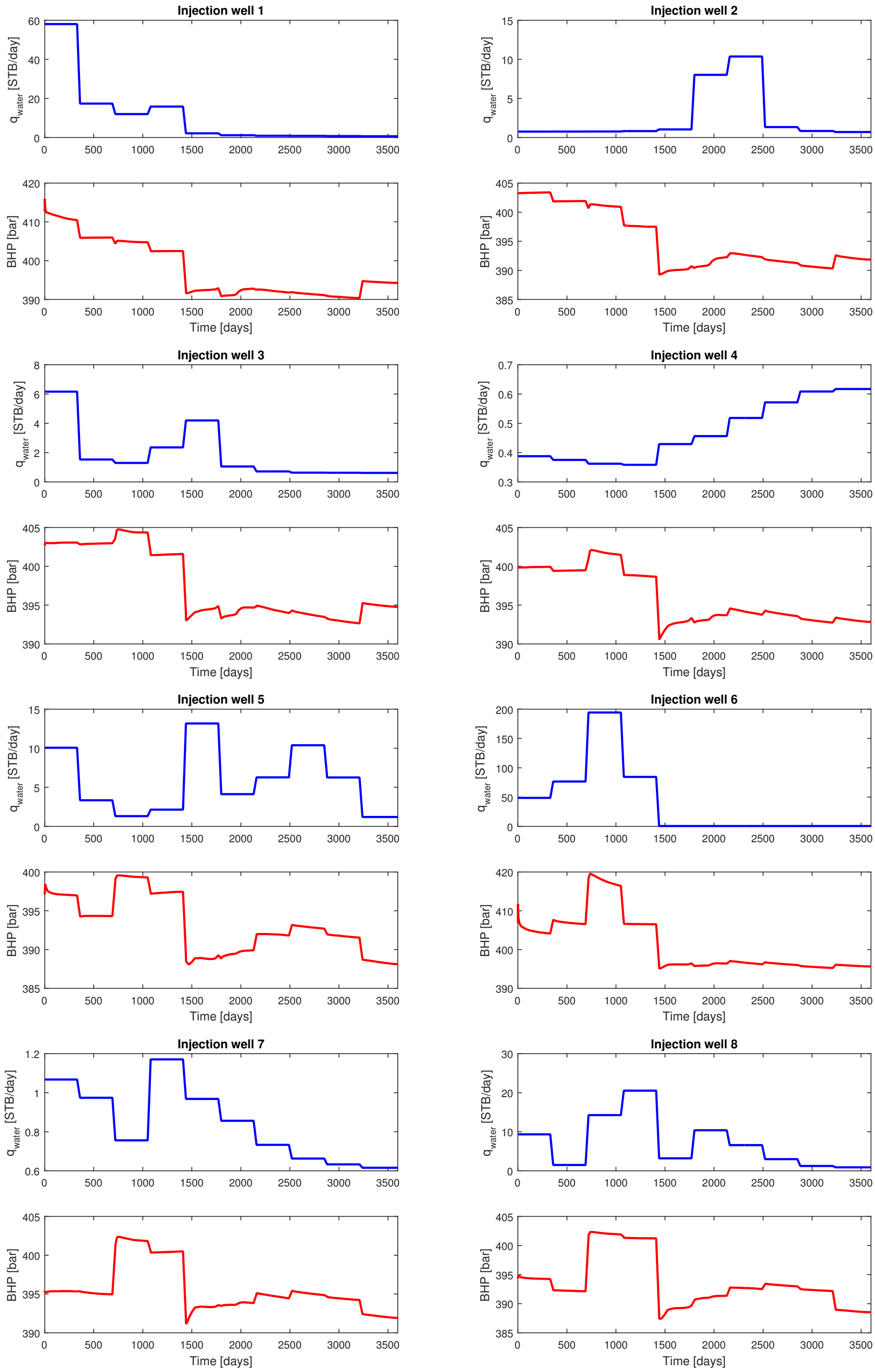

Figure B.2: Unconstrained output plot from the eight injectors

B.2 Extended results from Section 5.2.2

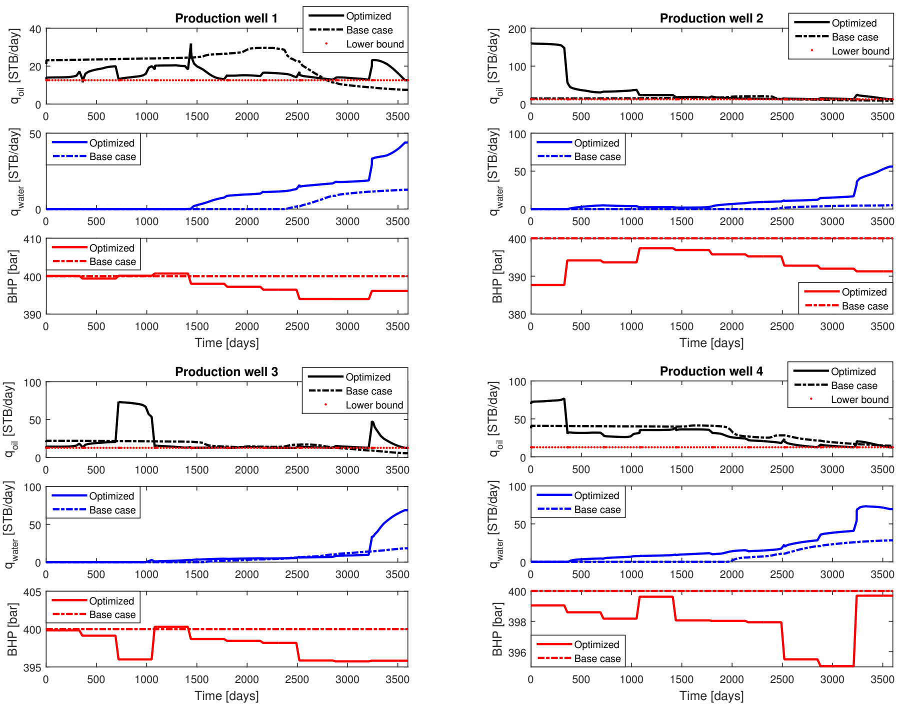

Figure B.3: Constrained output plot from the four producers

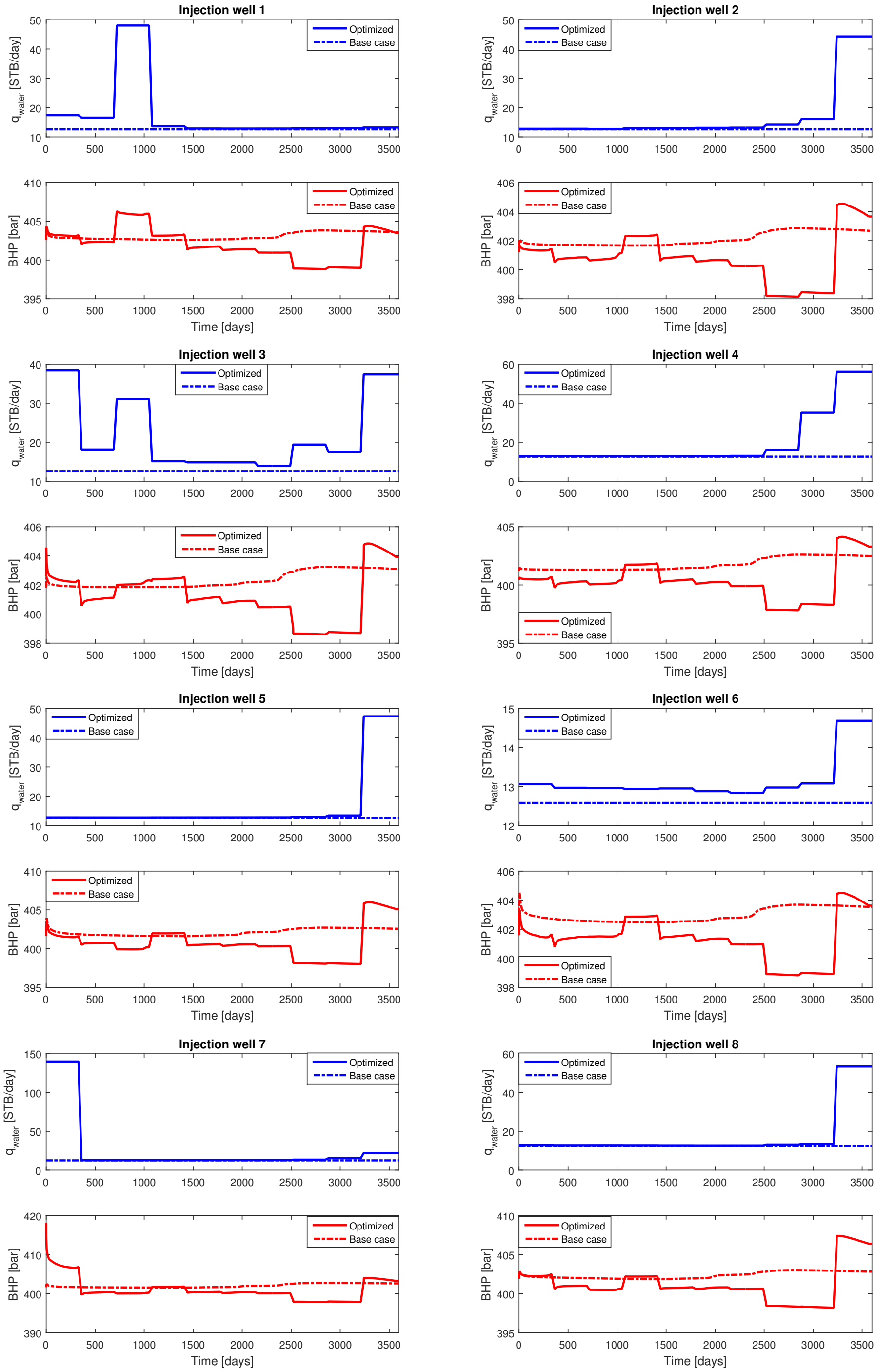

Figure B.4: Constrained output plot from the eight injectors

B.3 Extended results from Section 5.3.1

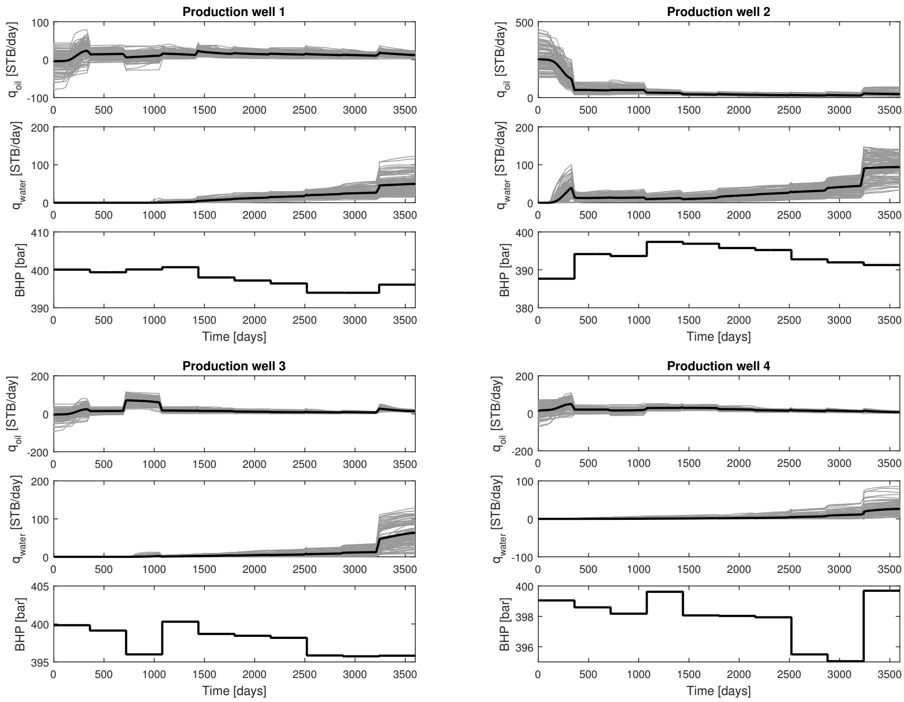

Figure B.5: Production scenarios with the deterministic solution

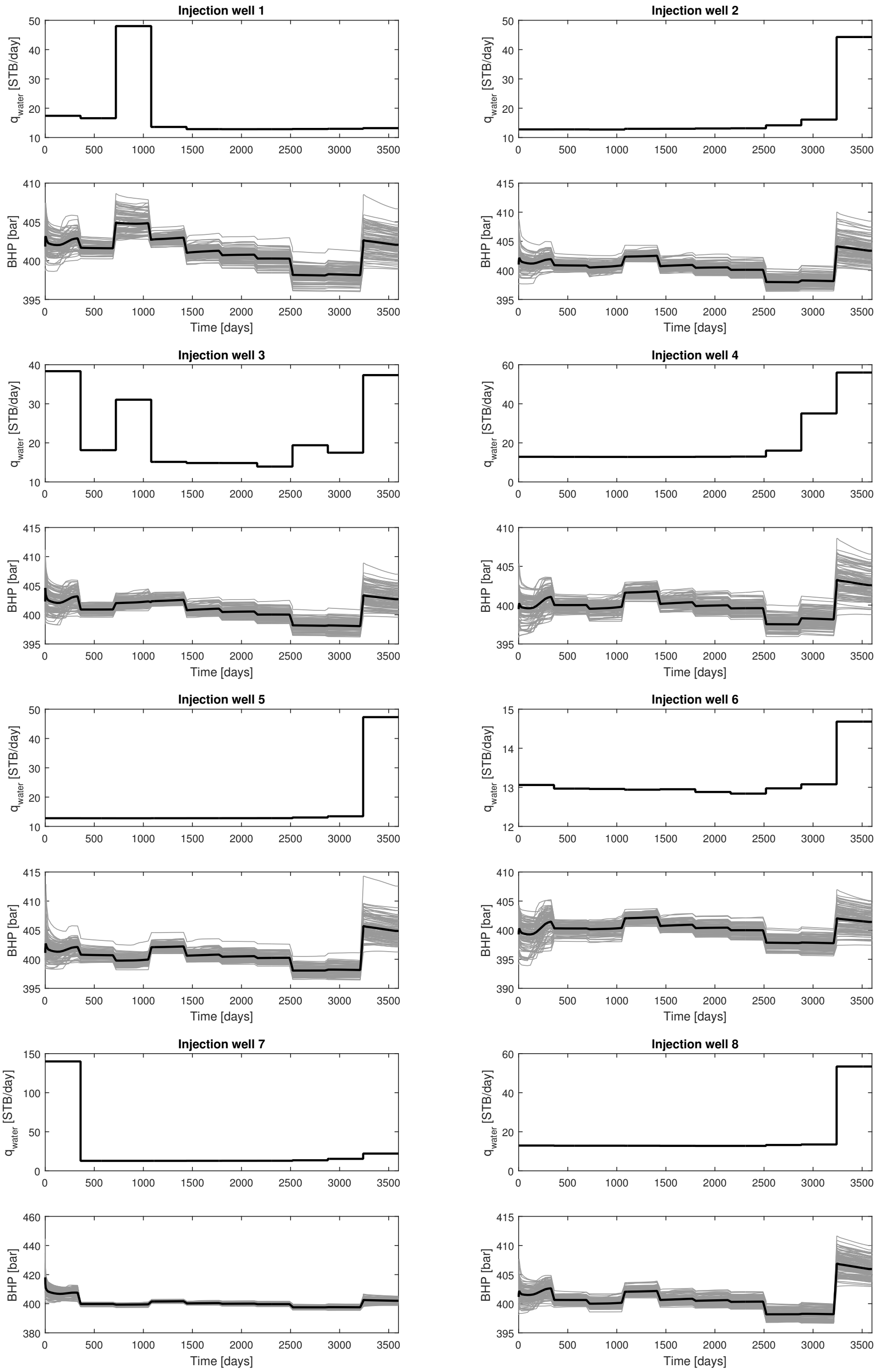

Figure B.6: Injection scenarios with the deterministic solution

B.4 Extended results from Section 5.3.2

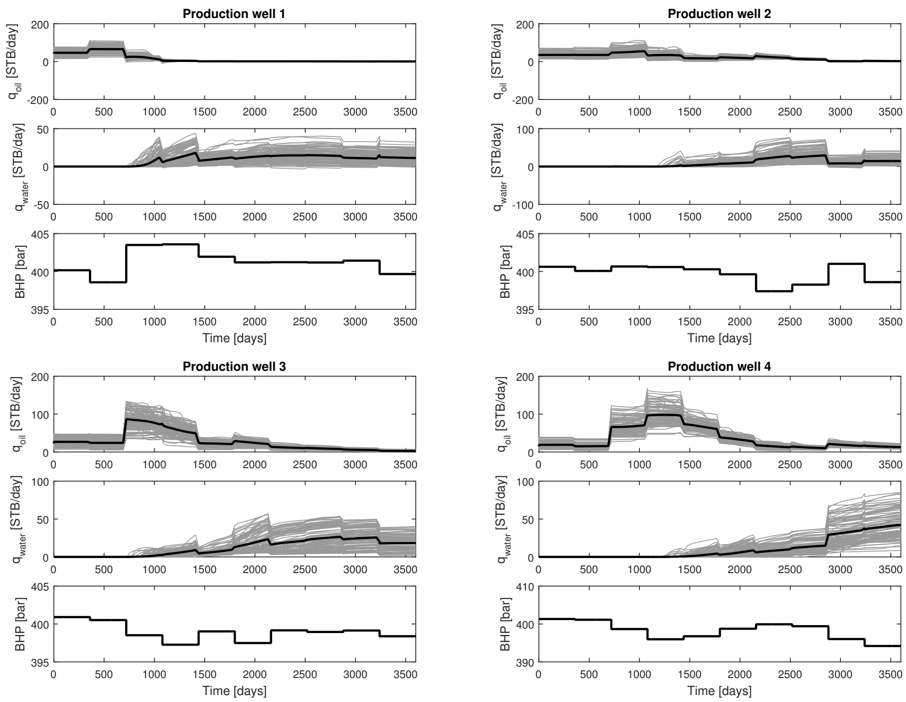

Figure B.7: Production scenarios with the robust solution

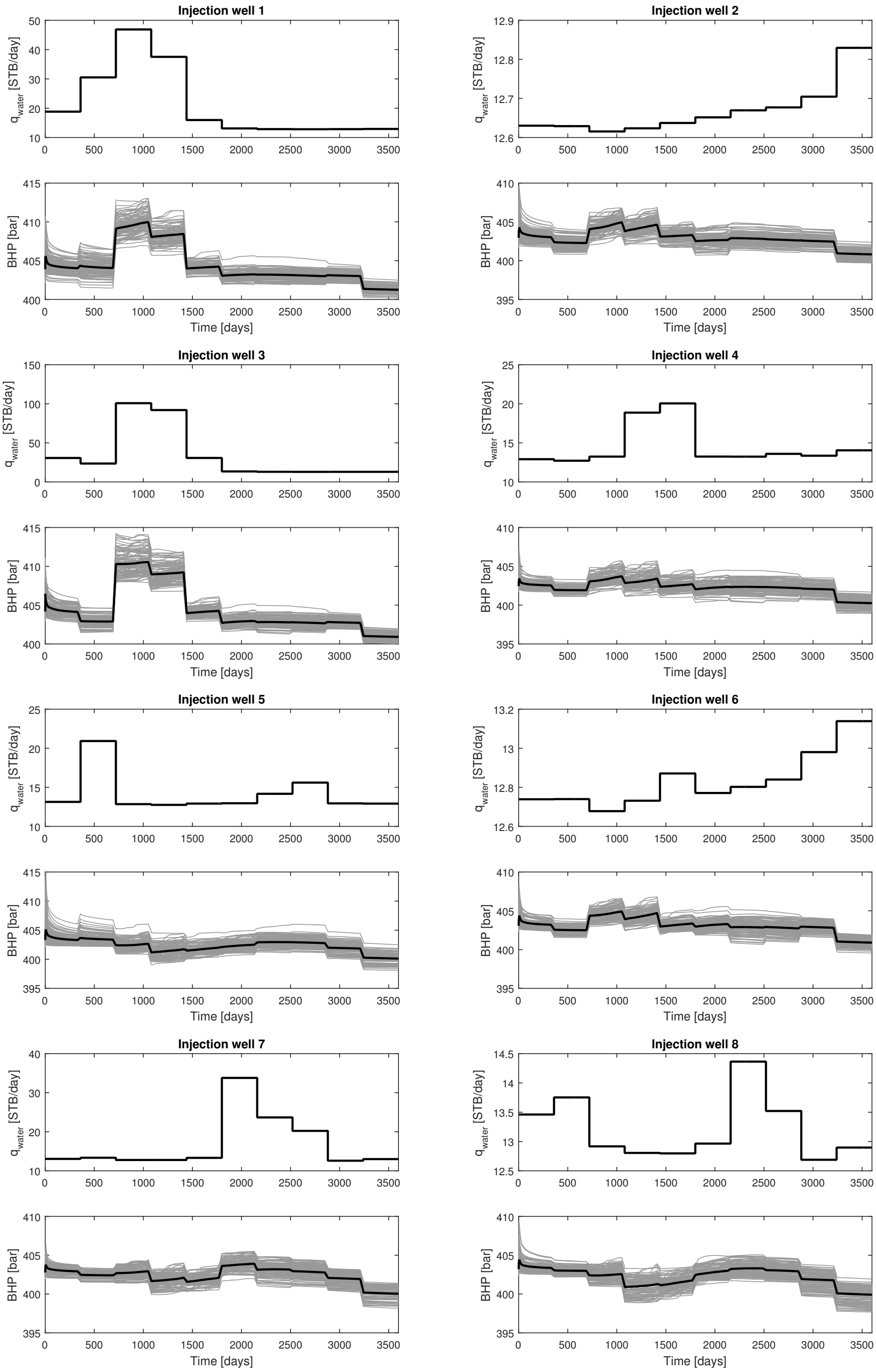

Figure B.8: Injection scenarios with the robust solution

Bibliography

Aanonsen, S., a.L. Eide, Holden, L., and Aasen, J. (1995). Optimizing Reservoir Performance Under Uncertainty with Application to Well Location. *Proceedings of SPE Annual Technical Conference and Exhibition*, pages 67–76.

Adamson, G. and Crick, M. (1996). Simulation throughout the life of a reservoir. *Oilfield Review*, pages 16–27.

Artzner, P., Delbaen, F., Eber, J.-M., and Heath, D. (1999). Coherent Measures of Risk. *Mathematical Finance*, 9(3):203–228.

Brouwer, D. and Naevdal, G. (2004). Improved Reservoir Management Through Optimal Control and Continuous Model Updating. In *Proceedings of SPE Annual Technical Conference and Exhibition*. Society of Petroleum Engineers.

Capolei, A., Suwartadi, E., Foss, B., and Bagterp Jørgensen, J. (2014). A Mean-Variance Objective for Robust Production Optimization in Uncertain Geological Scenarios. *Journal of Petroleum Science and Engineering*.

Chen, Z., Huan, G., and Ma, Y. (2006). *Computational Methods for Multiphase Flows in Porous Media*. SIAM.

Codas, A., Foss, B., and Camponogara, E. (2015). Output Constraint Handling & Parallelization for Oil Reservoir Control Optimization via Multiple Shooting. *SPE Journal*, Preprint(Preprint).

Corre, B., Thore, P., Feraudy, V. D., Vincent, G., and Elf, T. (2000). SPE 65205 Integrated Uncertainty Assessment For Project Evaluation and Risk Analysis. In *SPE European Petroleum Conference*, Paris, France. Society of Petroleum Engineers.

Da Cruz, P., Horne, R., and Deutsch, C. (2004). The Quality Map: A Tool for Reservoir Uncertainty Quantification and Decision Making. *SPE Reservoir Evaluation & Engineering*, 7:3–6.

Deutsch, C. and Srinivasan, S. (1996). Improved Reservoir Management Through Ranking Stochastic Reservoir Models. In *Proceedings of SPE/DOE Improved Oil Recovery Symposium*, pages 105–113. Society of Petroleum Engineers.

Evensen, G. (2003). The Ensemble Kalman Filter: Theoretical formulation and practical implementation. *Ocean Dynamics*, 53:343–367.

Foss, B. (2012). Real-Time Production Optimization and Reservoir Management at the IO Center. *IFAC Proceedings Volumes*, 1:7–12.

Foss, B. and Jensen, J. P. (2011). Performance Analysis for Closed-Loop Reservoir Management. *SPE Journal*, 16.

Frank Jahn, Mark Cook, M. G. (2008). *Hydrocarbon Exploration & Production*. Elsevier, 2nd edition.

Goel, V. and Grossmann, I. E. (2004). A stochastic programming approach to planning of offshore gas field developments under uncertainty in reserves. *Computers & Chemical Engineering*, 28(8):1409–1429.

Hanssen, K. G., Foss, B., and Teixeira, A. (2014). Production Optimization under Uncertainty with Constraint Handling.

Ioannou, P. a., Sun, J., and List, P. (1996). *Robust Adaptive Control*. Pearson Education, Inc.

Jansen, J. D. (2011). Adjoint-based optimization of multi-phase flow through porous media - A review. *Computers and Fluids*, 46(1):40–51.

Jansen, J. D., Essen, G. M. V., Hof, P. M. J. Van denFonseca, R. M., Kahrobaei, S., and Siraj, M. M. (2014). The egg model – a geological ensemble for reservoir simulation. *Geoscience Data Journal*, 56 Suppl 1.

Jonsbråten, T. (1998). Oil Field Optimization under Price Uncertainty. *Journal of the Operational Research Society*, 49(8):811–818.

Krogstad, S., Lie, K.-A., Mø yner, O., Nilsen, H. M. l., Raynaud, X., and Skaflestad, B. r. (2015). An Open-Source Framework for Rapid Prototyping and Evaluation of Reservoir Simulation Problems. In *SPE Reservoir Simulation Symposium*. Society of Petroleum Engineers.

Lie, K.-A. (2014). *An Introduction to Reservoir Simulation Using MATLAB*. SINTEF ICT, Department of Applied Mathematics, Oslo, Norway.

Lie, K.-A. and Mallison, B. T. (2013). Mathematical Models for Oil Reservoir Simulation. In Engquist, B., editor, *Encyclopedia of Applied and Computational Mathematics*. Springer-Verlag Berlin Heidelberg.

Lorentzen, R., Shafieirad, A., and Naevdal, G. (2009). Closed Loop Reservoir Management Using the Ensemble Kalman Filter and Sequential Quadratic Programming. *Proceedings of SPE Reservoir Simulation Symposium*.

Midttun, L. (2014). *Stochastic Programming Applied to Oil and Gas Systems*. Project work, Norwegian University of Science and Technology.

Nolen-Hoeksema, R. (2014). Defining Permeability. *Oilfield Review*.

Peters, L., Arts, R., Brouwer, G., Geel, C., Cullick, S., Lorentzen, R., Chen, Y., Dunlop, N., Vossepoel, F., Xu, R., Sarma, P., Alhuthali, A., and Reynolds, A. (2010). Results of the Brugge Benchmark Study for Flooding Optimization and History Matching. *SPE Reservoir Evaluation & Engineering*, 13(June).

Seborg, D. E., Edgar, T. F., Mellichamp, D. A., and Doyle, F. J. (2011). *Process Dynamics and Control*. John Wiley & Sons, Inc., 3rd edition.

Shapiro, A. and Philpott, A. (2007). A Tutorial on Stochastic Programming. Technical report, School of Industrial and Systems Engineering, Georgia Institute of Technology, Atlanta, Georgia.

Smithson, T. (2012). Defining Porosity. *Oilfield Review*.

Tarhan, B., Grossmann, I. E., and Goel, V. (2009). Stochastic Programming Approach for the Planning of Offshore Oil or Gas Field Infrastructure under Decision-Dependent Uncertainty. *Industrial & Engineering Chemistry Research*, 48(6):3078–3097.

Van Essen, G., Rezapour, A., Van Den Hof, P., and Jansen, J. (2010). Integrated dynamic optimization and control in reservoir engineering using locally identified linear models. In *2010 49th IEEE Conference on Decision and Control (CDC)*, pages 7643–7648. IEEE.

Van Essen, G., Zandvliet, M., Van den Hof, P., Bosgra, O., and Jansen, J.-D. (2009). Robust Waterflooding Optimization of Multiple Geological Scenarios. *SPE Journal*, 14(01):202–210.

Wang, C., Li, G., and Reynolds, A. C. (2009). Production Optimization in Closed-Loop Reservoir Management. *SPE Journal*, 14(3).

White, F. M. (2003). *Fluid Mechanics*. McGraw-Hill, New York, United States, 5th edition.

Zafari, M. and Reynolds, A. (2005). Assessing the Uncertainty in Reservoir Description and Performance Predictions With the Ensemble Kalman Filter. In *SPE Annual Technical Conference and Exhibition*, number September, Dallas, Texas.